A **halo model** approach to describe clustering and emission of the **two** main star-forming **galaxy populations** for Cosmic Infrared Background studies

SEMAINE DE L'ASTROPHYSIQUE FRANÇAISE

Grenoble

Giorgia Zagatti,
Erminia Calabrese, Caterina Chiocchetta, Martina Gerbino, Mattia Negrello, Luca Pagano

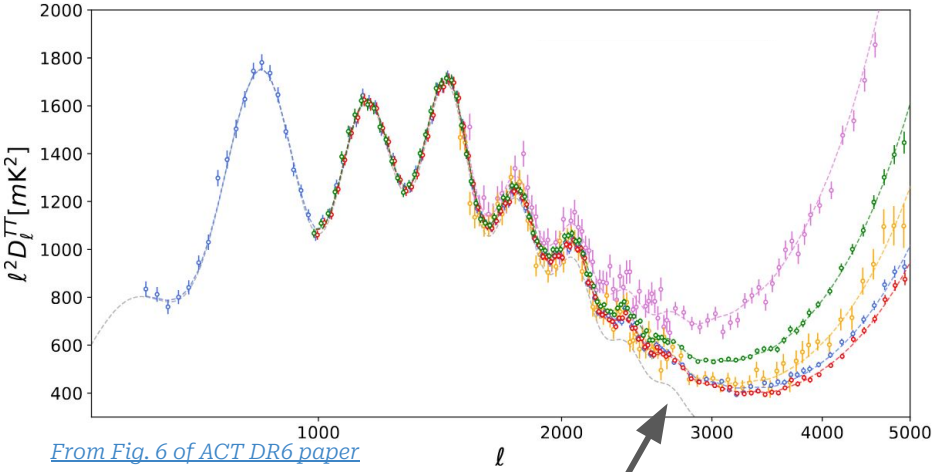

From Fig. 6 of ACT DR6 paper

High ℓ analysis ↓ cosmic variance

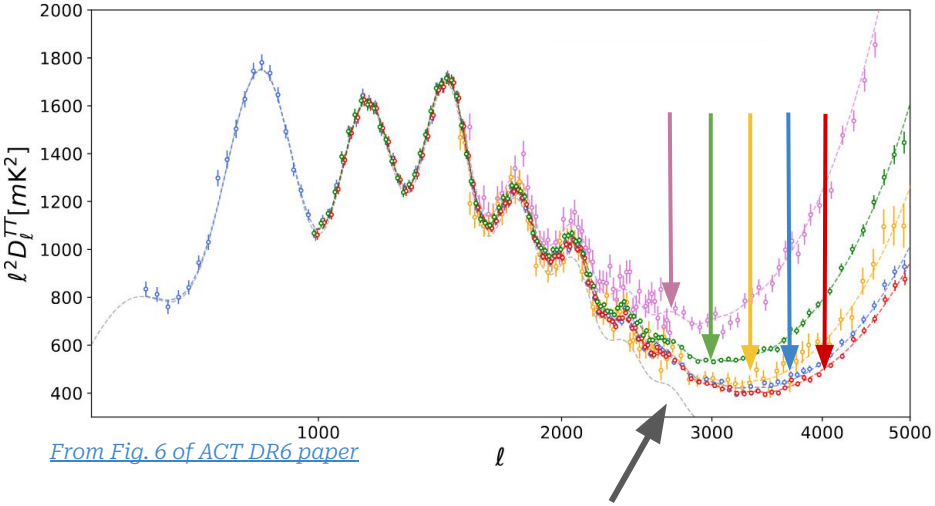

From Fig. 6 of ACT DR6 paper

High ℓ analysis

↓ cosmic variance

↑ foregrounds contamination

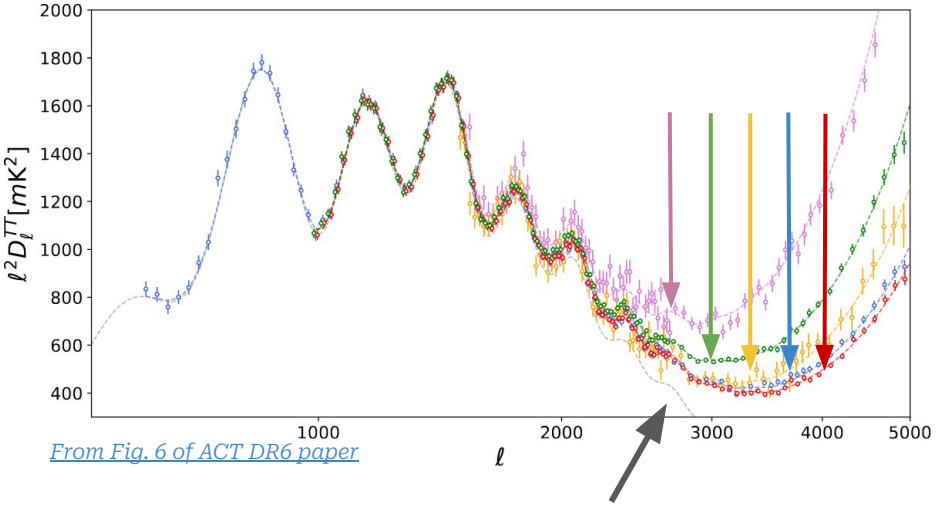

From Fig. 6 of ACT DR6 paper

High ℓ analysis

↓ cosmic variance

↑ foregrounds contamination

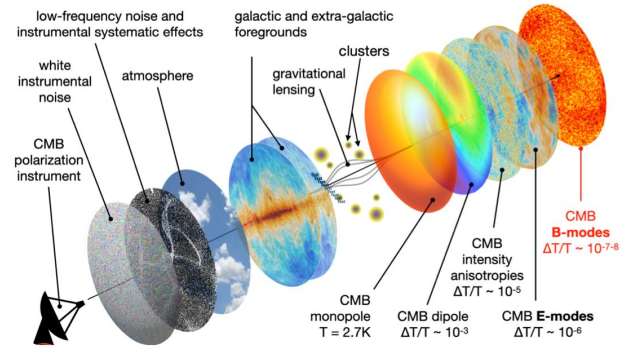

Contaminants of the primary CMB signal

clean CMB signal and extract information from the early Universe

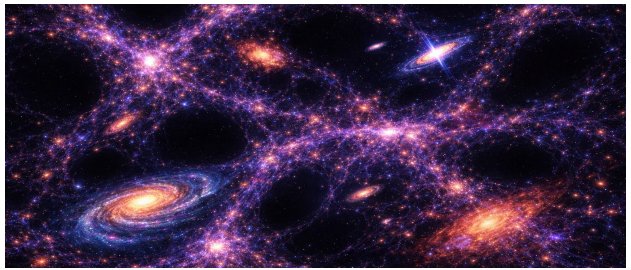

Tracers of the matter density field

clustering studies, formation and evolution of the LSS, and information on astrophysical processes

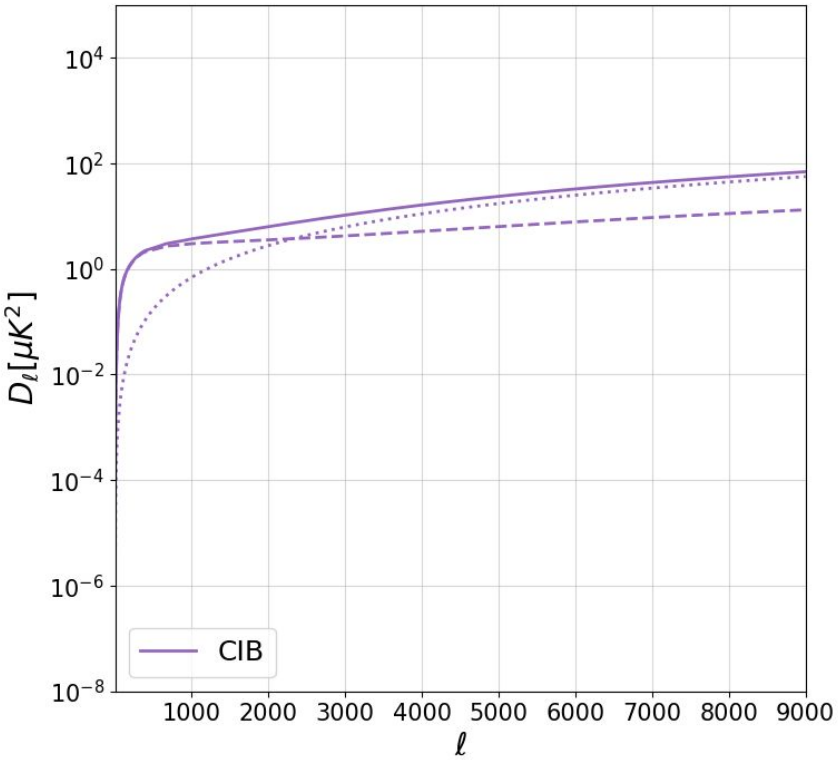

Cosmic Infrared Background
from Dusty Star-Forming Galaxies

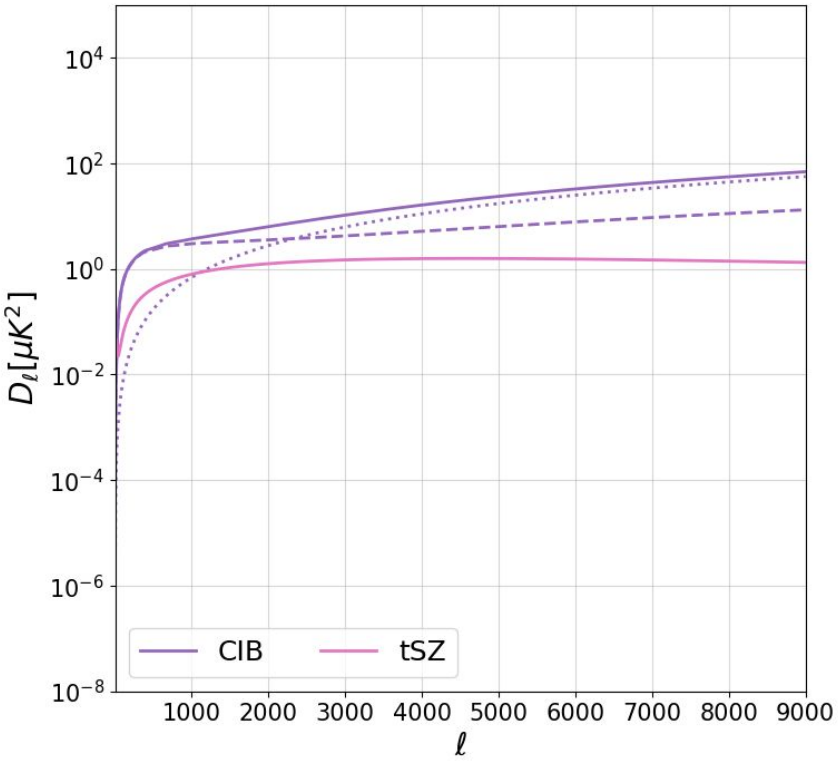

Cosmic Infrared Background
from Dusty Star-Forming Galaxies

thermal Sunyaev-Zel'dovich
from hot gas in galaxy clusters

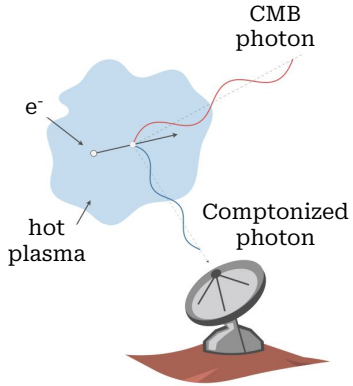

Credits: Carlstrom et al. (2002)

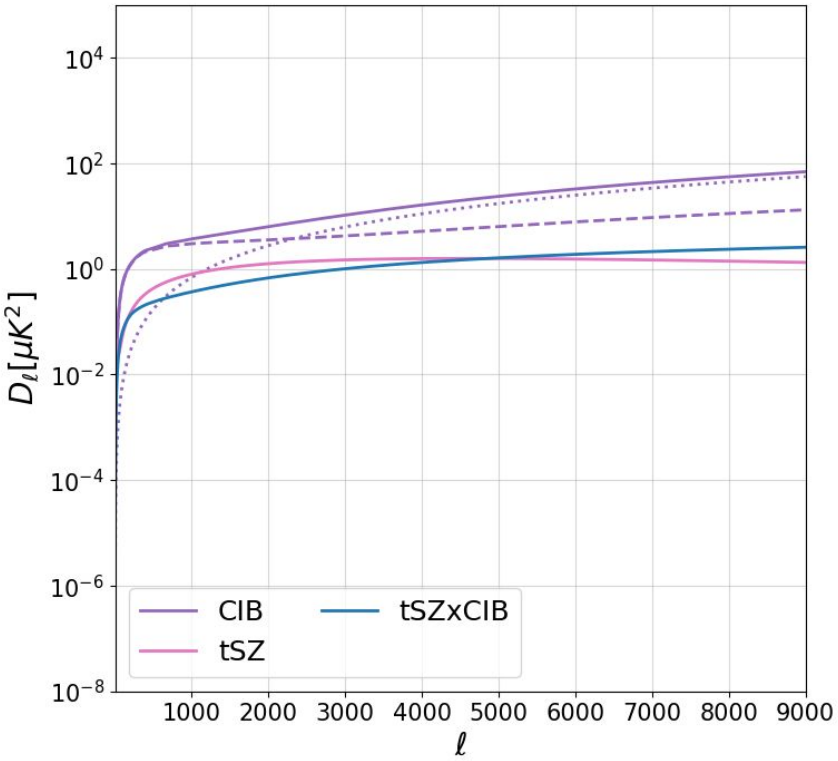

Cosmic Infrared Background
from Dusty Star-Forming Galaxies

thermal Sunyaev-Zel'dovich
from hot gas in galaxy clusters

tSZ x CIB
they trace the same matter distribution

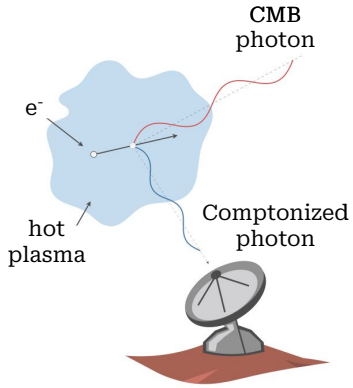

Credits: Carlstrom et al. (2002)

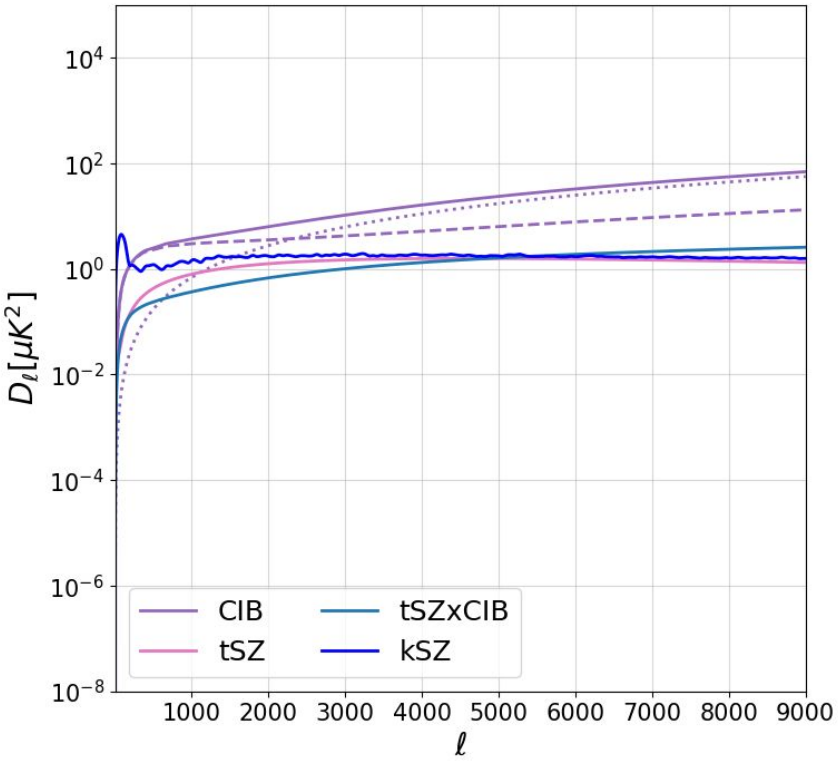

Cosmic Infrared Background
from Dusty Star-Forming Galaxies

thermal Sunyaev-Zel'dovich
from hot gas in galaxy clusters

tSZ x CIB
they trace the same matter distribution

kinetic Sunyaev-Zel'dovich
from the bulk velocity of hot gas in galaxy clusters

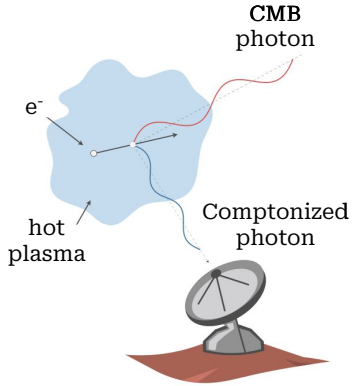

Credits: Carlstrom et al. (2002)

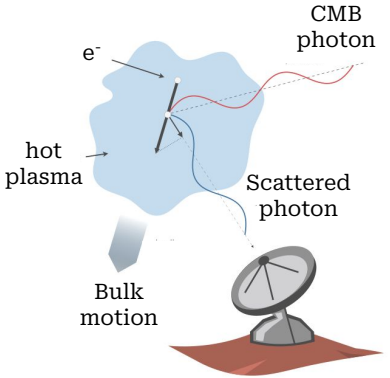

Credits: Carlstrom et al. (2002)

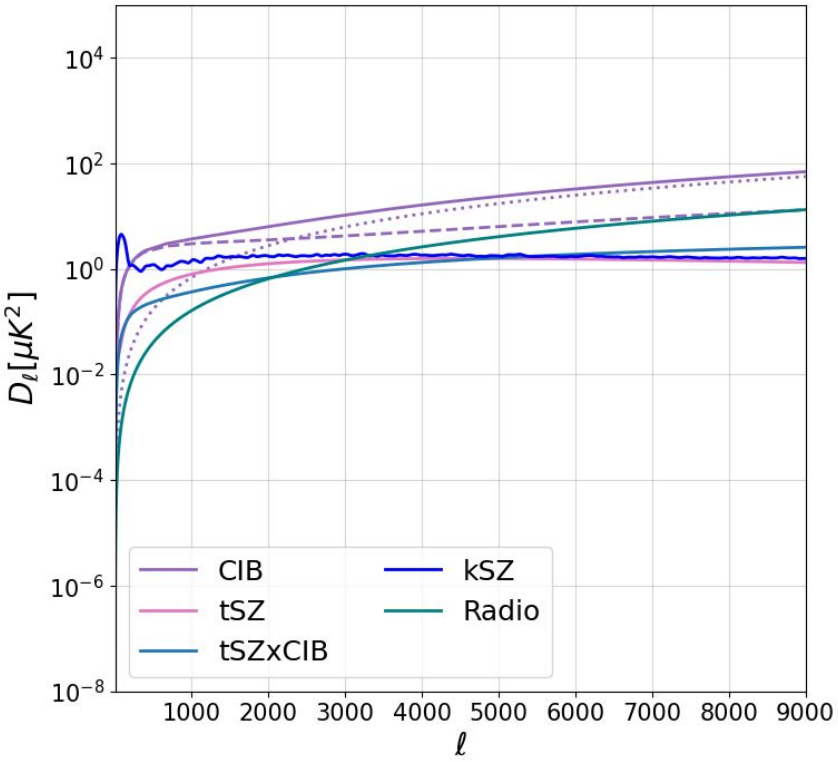

Cosmic Infrared Background
from Dusty Star-Forming Galaxies

thermal Sunyaev-Zel'dovich
from hot gas in galaxy clusters

tSZ x CIB
they trace the same matter distribution

kinetic Sunyaev-Zel'dovich
from the bulk velocity of hot gas in galaxy clusters

Radio sources
from AGN and radio loud galaxies

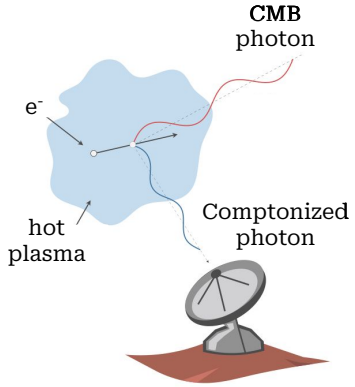

Credits: Carlstrom et al. (2002)

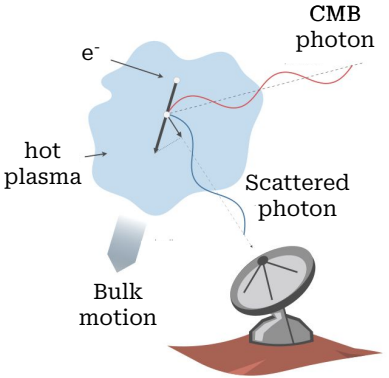

Credits: Carlstrom et al. (2002)

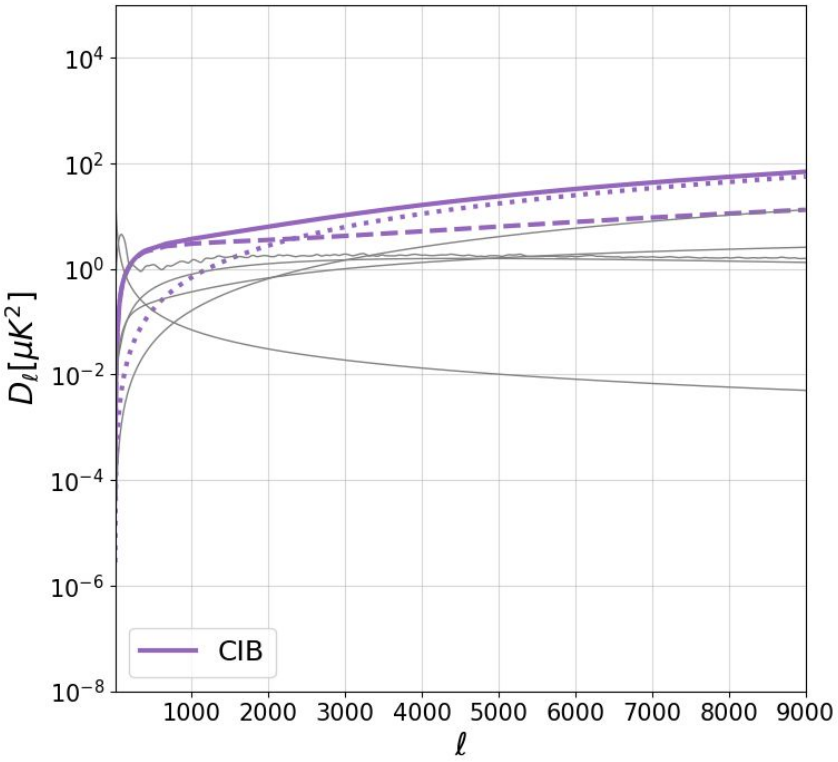

Cosmic Infrared Background
from Dusty Star-Forming Galaxies

thermal Sunyaev-Zel'dovich
from hot gas in galaxy clusters

tSZ x CIB
they trace the same matter distribution

kinetic Sunyaev-Zel'dovich
from the bulk velocity of hot gas in galaxy clusters

Radio sources
from AGN and radio loud galaxies

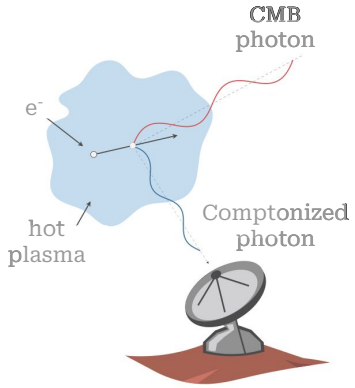

Credits: Carlstrom et al. (2002)

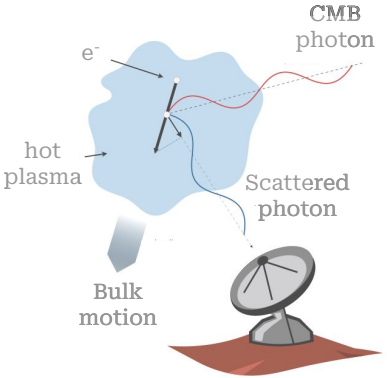

Credits: Carlstrom et al. (2002)

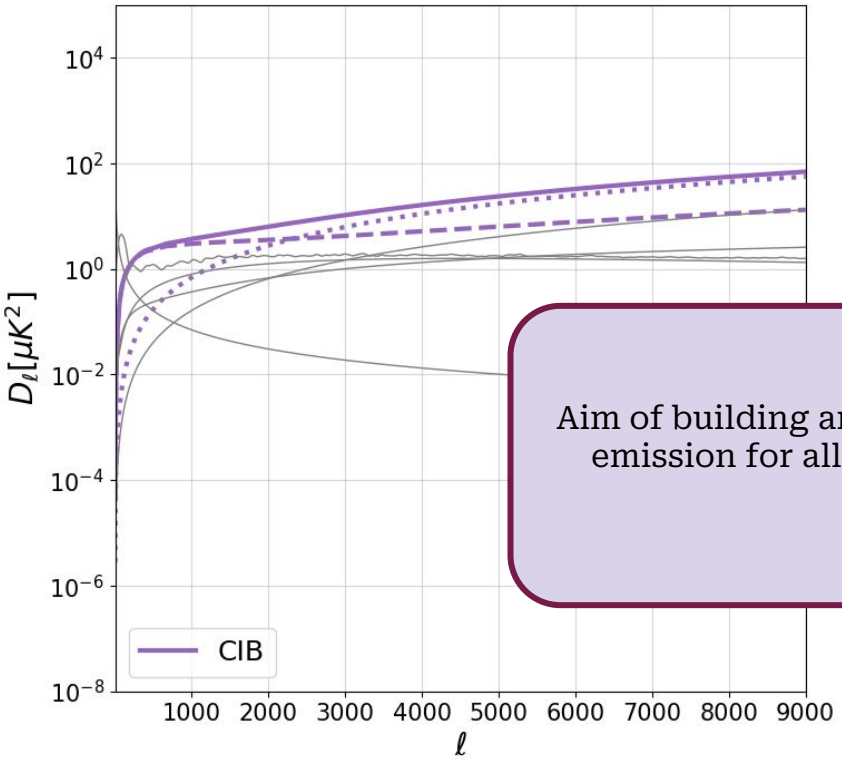

Cosmic Infrared Background
from Dusty Star-Forming Galaxies

thermal Sunyaev-Zel'dovich
from hot gas in galaxy clusters

ter

ovich
t gas in

Radio sources
from AGN and radio loud galaxies

Aim of building an analytic model of the CIB emission for all frequencies and angular scales

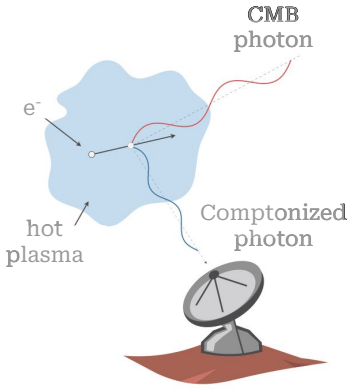

Credits: Carlstrom et al. (2002)

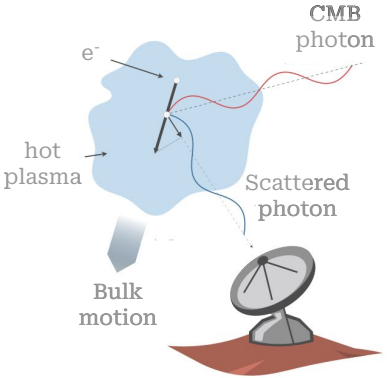

Credits: Carlstrom et al. (2002)

Halo Model : tool to predict non-linear matter (and its tracers) power spectrum

Cooray A., & Sheth R. (2002)

Halo Model : tool to predict non-linear matter (and its tracers) power spectrum

Cooray A., & Sheth R. (2002)

HOW?

All matter in the Universe is contained in virialized structures

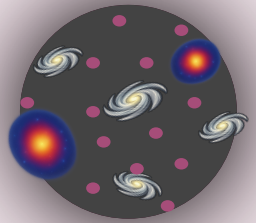

Dark matter haloes

1. Halo mass function
   Tinker et al. (2008)
2. Halo bias
   Tinker et al. (2010b)
3. Halo density profile
   Navarro et al. (1997)

Halo Model : tool to predict non-linear matter (and its tracers) power spectrum

Cooray A., & Sheth R. (2002)

All matter in the Universe is contained in virialized structures

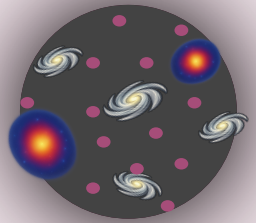

Dark matter haloes

HOW?

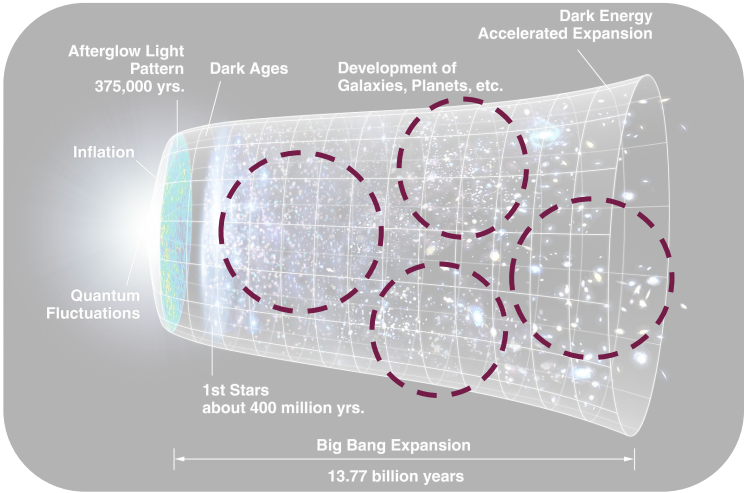

1. Halo mass function
   Tinker et al. (2008)
2. Halo bias
   Tinker et al. (2010b)
3. Halo density profile
   Navarro et al. (1997)

Halo Model : tool to predict non-linear matter (and its tracers) power spectrum

Cooray A., & Sheth R. (2002)

All matter in the Universe is contained in virialized structures

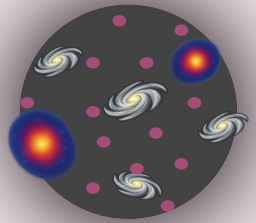

Dark matter haloes

HOW?

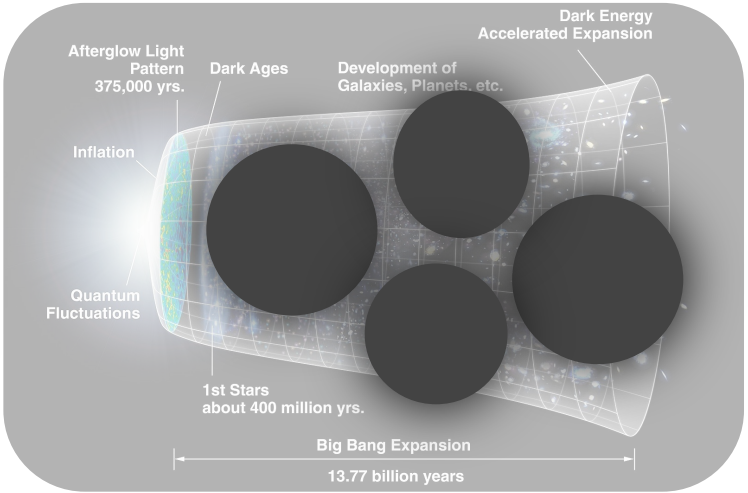

1. Halo mass function
   Tinker et al. (2008)
2. Halo bias
   Tinker et al. (2010b)
3. Halo density profile
   Navarro et al. (1997)

Halo Model : tool to predict non-linear matter (and its tracers) power spectrum

Cooray A., & Sheth R. (2002)

All matter in the Universe is contained in virialized structures

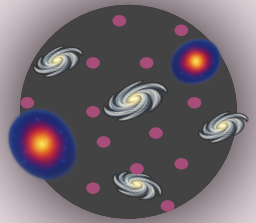

Dark matter haloes

HOW?

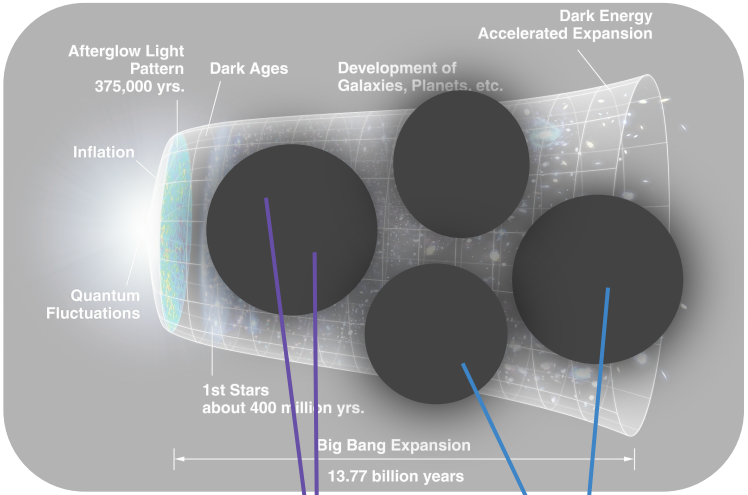

- Matter power spectrum

1. Halo mass function
   Tinker et al. (2008)
2. Halo bias
   Tinker et al. (2010b)
3. Halo density profile
   Navarro et al. (1997)

$$P_{uv}(k) = P_{uv}^{1h}(k) + P_{uv}^{2h}(k)$$

Halo Model : tool to predict non-linear matter (and its tracers) power spectrum

Cooray A., & Sheth R. (2002)

All matter in the Universe is contained in virialized structures

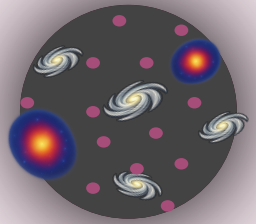

Dark matter haloes

1. Halo mass function
   Tinker et al. (2008)
2. Halo bias
   Tinker et al. (2010b)
3. Halo density profile
   Navarro et al. (1997)

HOW?

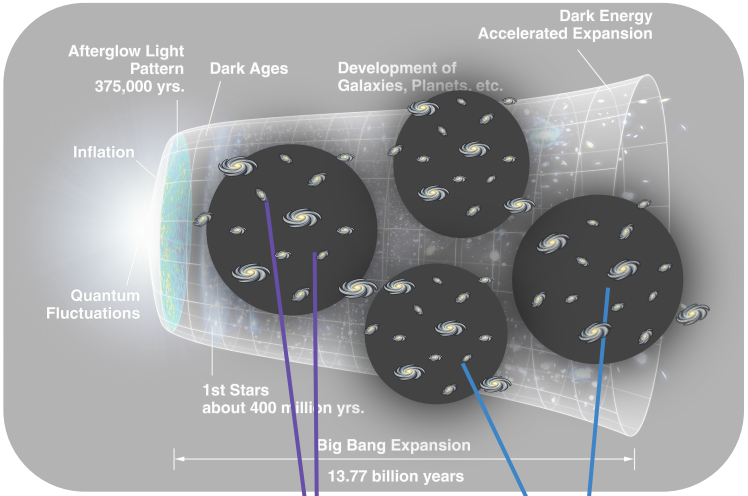

- Matter power spectrum
- Galaxy power spectrum

$$P_{uv}(k) = P_{uv}^{1h}(k) + P_{uv}^{2h}(k)$$

Halo Occupation Distribution

Tinker & Wetzel (2010)

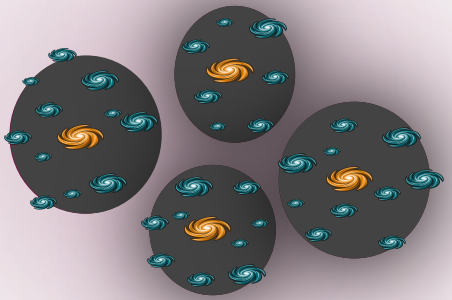

- **Central galaxies**

$$N_{\rm cent} = \frac{1}{2}\left[1 + {\rm erf}\left(\frac{\log M - \log M_{\rm min}}{\sigma_{\log M}}\right)\right]$$

- **Satellite galaxies**

$$N_{\rm sat} = \frac{1}{2}\left[1 + {\rm erf}\left(\frac{\log M - \log 2M_{\rm min}}{\sigma_{\log M}}\right)\right]\left(\frac{M}{M_{\rm sat}}\right)^{\alpha}$$

Halo Occupation Distribution

Tinker & Wetzel (2010)

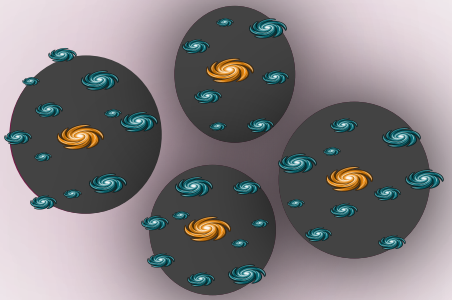

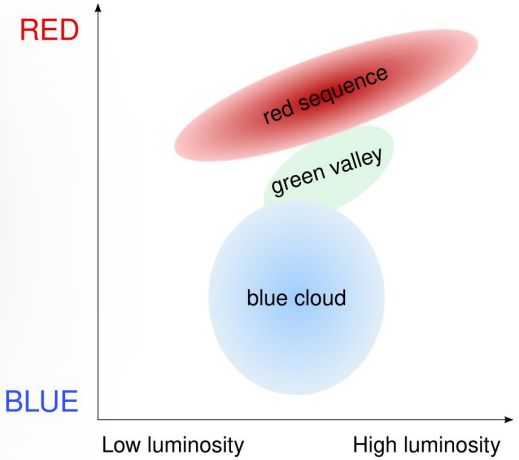

- **Central galaxies**

$$N_{\rm cent} = \frac{1}{2}\left[1 + {\rm erf}\left(\frac{\log M - \log M_{\rm min}}{\sigma_{\log M}}\right)\right]$$

- **Satellite galaxies**

$$N_{\rm sat} = \frac{1}{2}\left[1 + {\rm erf}\left(\frac{\log M - \log 2M_{\rm min}}{\sigma_{\log M}}\right)\right]\left(\frac{M}{M_{\rm sat}}\right)^{\alpha}$$

Single galaxy population models for CIB

Lagache et al. (2003)
Maniyar et al. (2018, 2021)
Viero et al. (2013)

Halo Occupation Distribution

Tinker & Wetzel (2010)

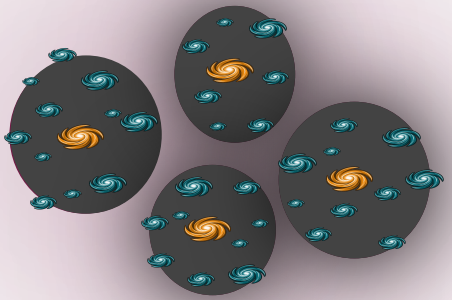

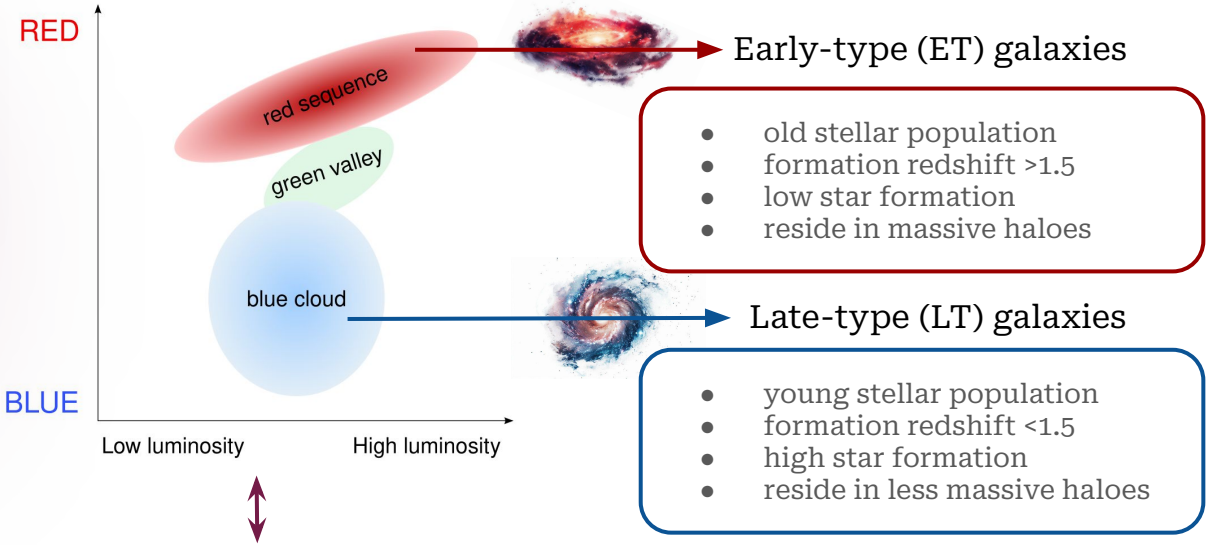

- **Central galaxies**

$$N_{\rm cent} = \frac{1}{2}\left[1 + {\rm erf}\left(\frac{\log M - \log M_{\rm min}}{\sigma_{\log M}}\right)\right]$$

- **Satellite galaxies**

$$N_{\rm sat} = \frac{1}{2}\left[1 + {\rm erf}\left(\frac{\log M - \log 2M_{\rm min}}{\sigma_{\log M}}\right)\right]\left(\frac{M}{M_{\rm sat}}\right)^{\alpha}$$

Single galaxy population models for CIB

Lagache et al. (2003)
Maniyar et al. (2018, 2021)
Viero et al. (2013)

$$P_{gal}(k) = P_{gal}^{ET}(k) + P_{gal}^{LT}(k) + P_{gal}^{ET\times LT}(k)$$

Zagatti et al. 2024

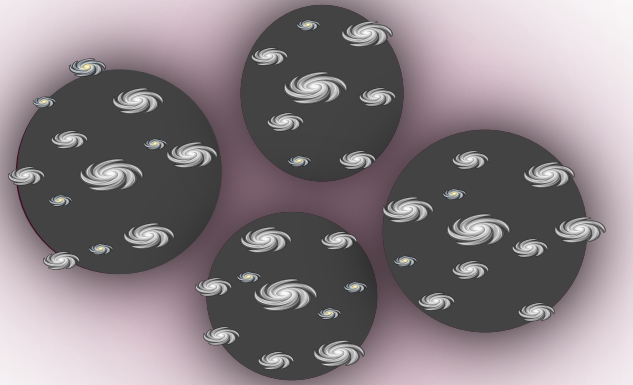

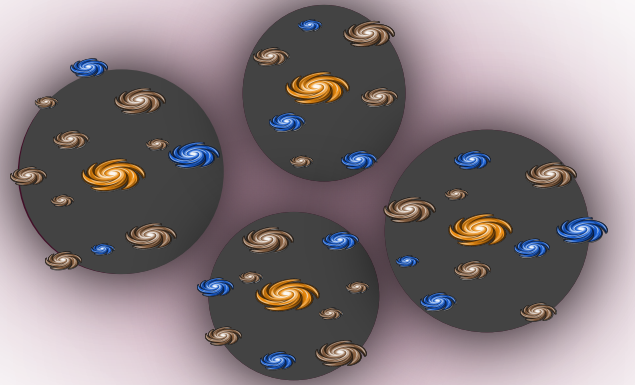

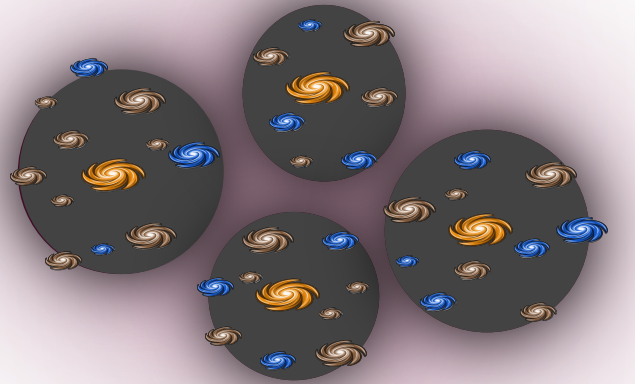

Emissivity function *(luminosity function)*

$$j_\nu(z)$$

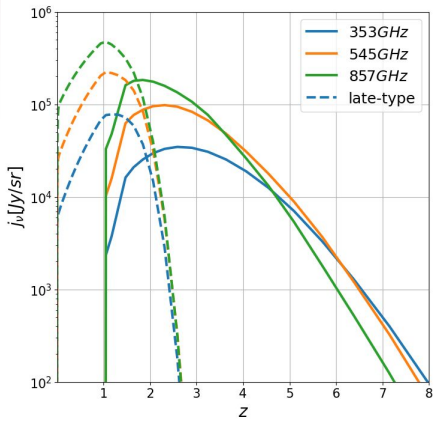

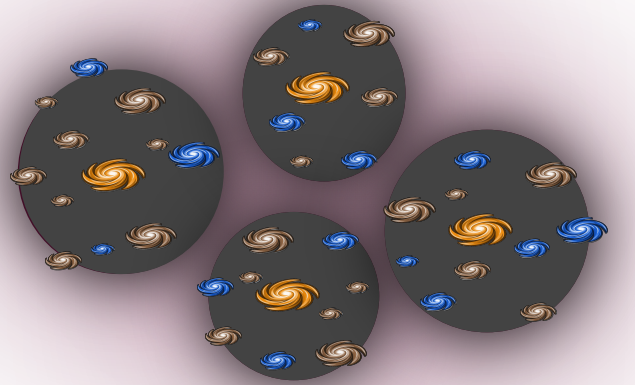

$$C_{\ell,\nu\times\nu\prime}^{CIB} = C_{\ell,\nu\times\nu\prime}^{\mathrm{clust}} + C_{\ell,\nu\times\nu\prime}^{SN}$$

- **Clustering term**

$$C_{\ell,\nu\times\nu\prime}^{\mathrm{clust}} = \int \frac{dz}{\chi^2}\frac{dz}{d\chi} j_\nu(z) j_{\nu\prime}(z) P_{\mathrm{gal}}$$

Emissivity function *(luminosity function)*

$$j_\nu(z)$$

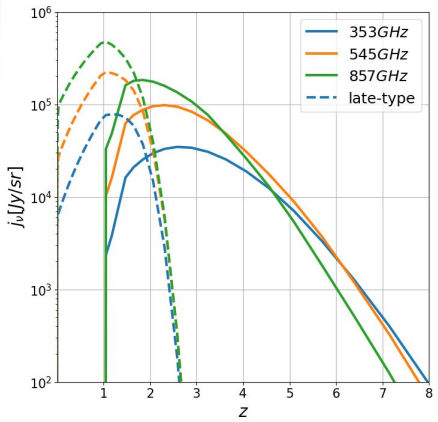

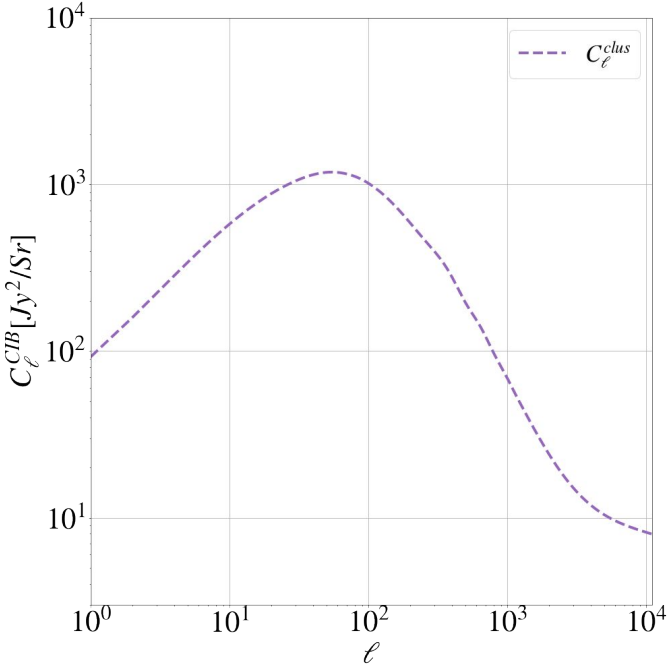

$$C_{\ell,\nu\times\nu\prime}^{CIB} = C_{\ell,\nu\times\nu\prime}^{\rm clust} + C_{\ell,\nu\times\nu\prime}^{SN}$$

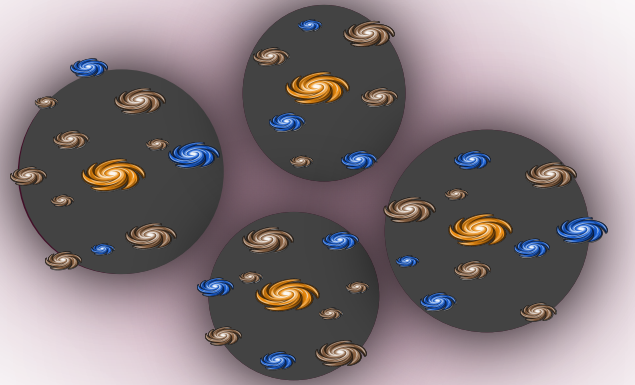

- **Clustering term**

$$C_{\ell,\nu\times\nu\prime}^{\rm clust} = \int \frac{dz}{\chi^2}\frac{dz}{d\chi} j_\nu(z) j_{\nu\prime}(z) P_{\rm gal}$$

- **Shot Noise term**

$$C_{\ell,\nu}^{SN} = \int_0^{S_\nu^{\rm lim}} S_\nu^2 \frac{d^2N(S_\nu)}{dS_\nu d\Omega} dS_\nu$$

Emissivity function *(luminosity function)*

$$j_\nu(z)$$

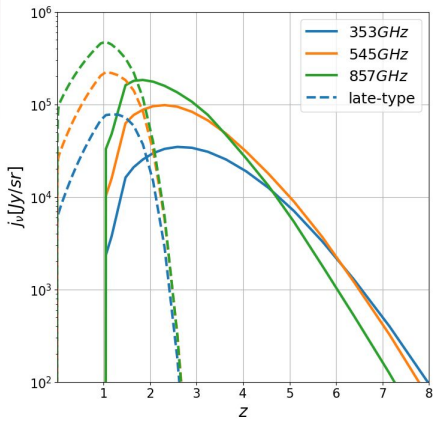

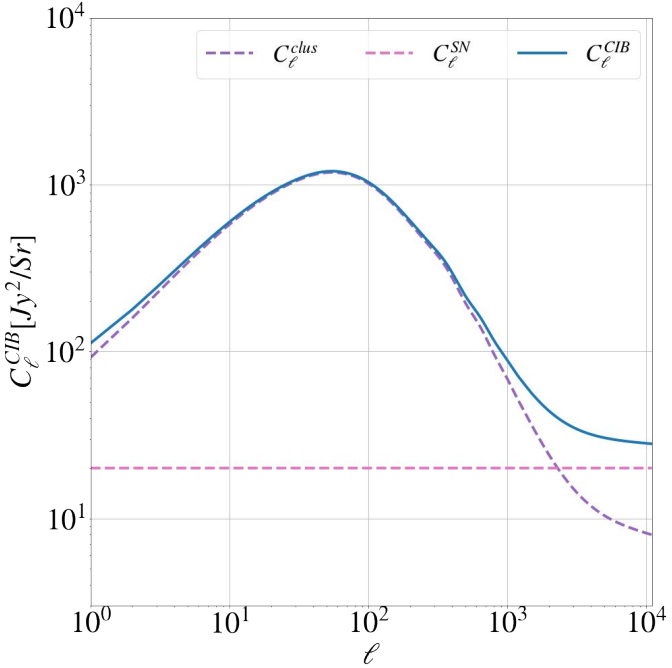

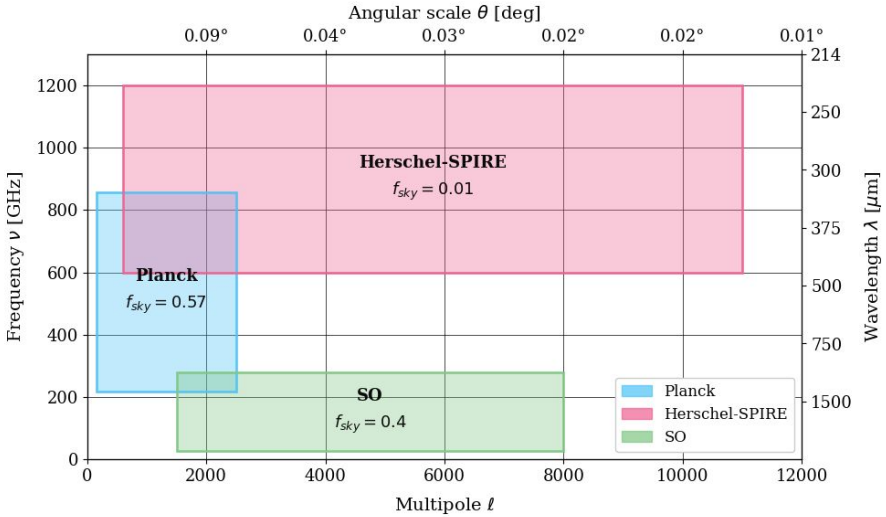
Angular scale θ [deg]
0.09°
0.04°
0.03°
0.02°
0.02°
0.01°
Frequency ν [GHz]
Wavelength λ [μm]
Herschel-SPIRE
$f_{sky} = 0.01$
Planck
$f_{sky} = 0.57$
SO
$f_{sky} = 0.4$
Planck
Herschel-SPIRE
SO
Multipole ℓ

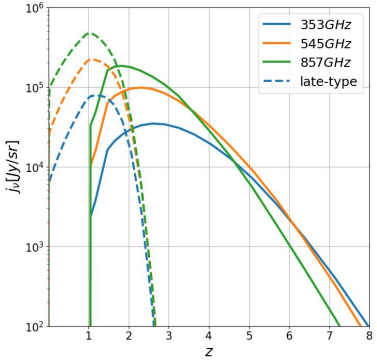
353GHz
545GHz
857GHz
late-type
z

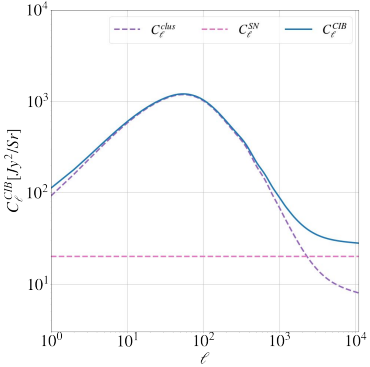
C_ℓ^{clus}
C_ℓ^{SN}
C_ℓ^{CIB}
$C_\ell^{CIB}[Jy^2/Sr]$
ℓ

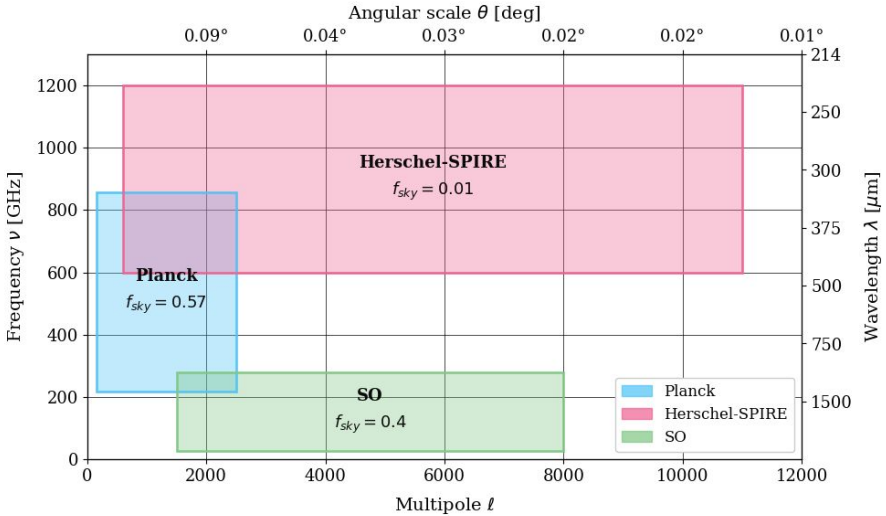

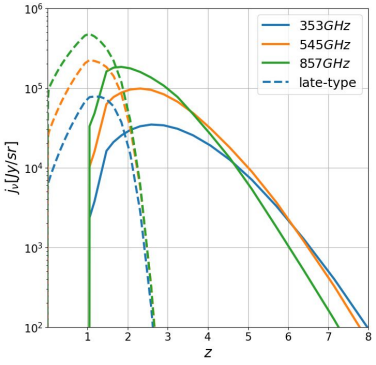

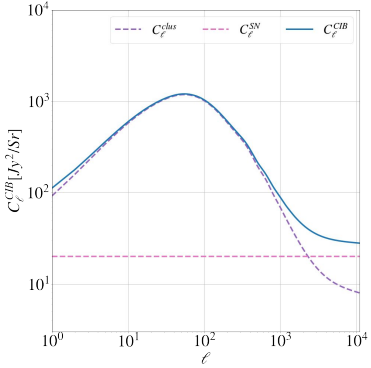

Planck **(P14)**	Planck-Lenz analysis **(L19)**	Herschel-SPIRE **(V19)**

Dataset	**Frequency channels** (GHz)	**Multipole range**
P14	217, 353, 545, 857	150-2500
L19	353, 545, 857	75-2500
V19	600, 857, 1200	600-11000

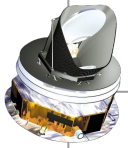

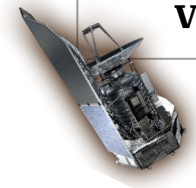

- Different frequencies are sensitive to different galaxy populations
- Different scales are sensitive to different power spectrum components

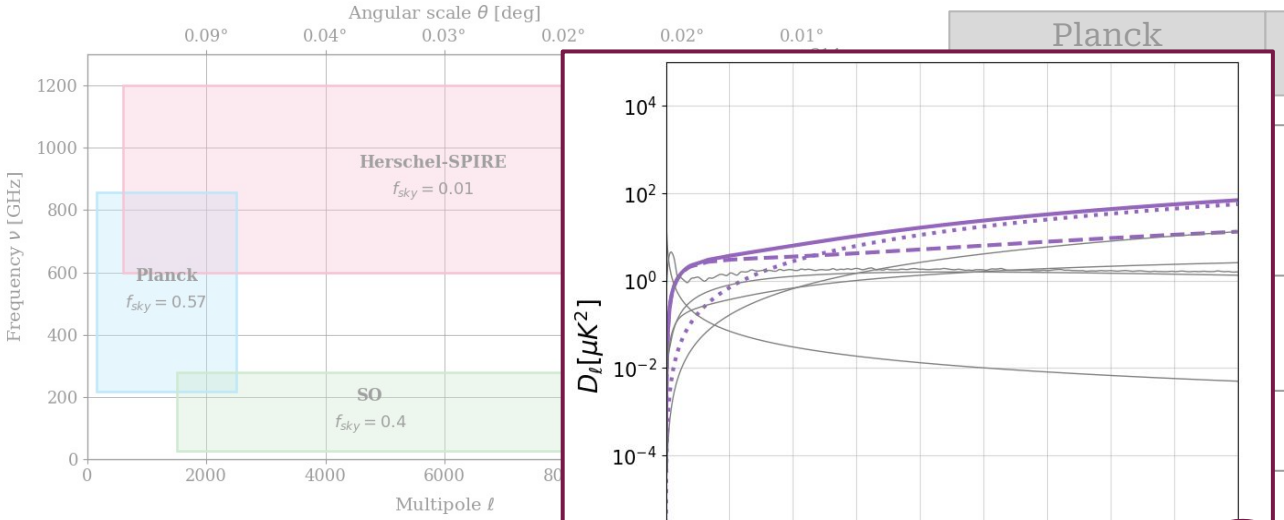

Planck	Planck-Lenz analysis **(L19)**	Herschel-SPIRE **(V19)**

	Frequency channels (GHz)	**Multipole range**
	217, 353, 545, 857	150-2500
	353, 545, 857	75-2500
	600, 857, 1200	600-11000

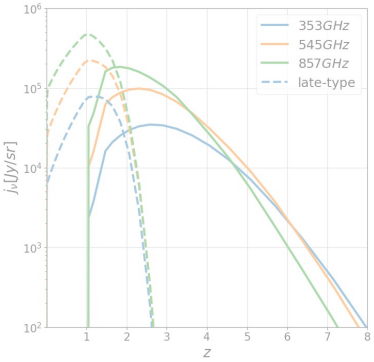

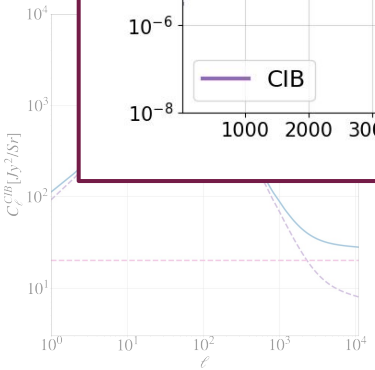

$$\log M_{min}^{ET}$$
$$\log M_{min}^{LT}$$
$$\alpha_{ET}$$
$$\alpha_{LT}$$

- uencies are sensitive to different ations
- scales are sensitive to different power spectrum components

Planck data

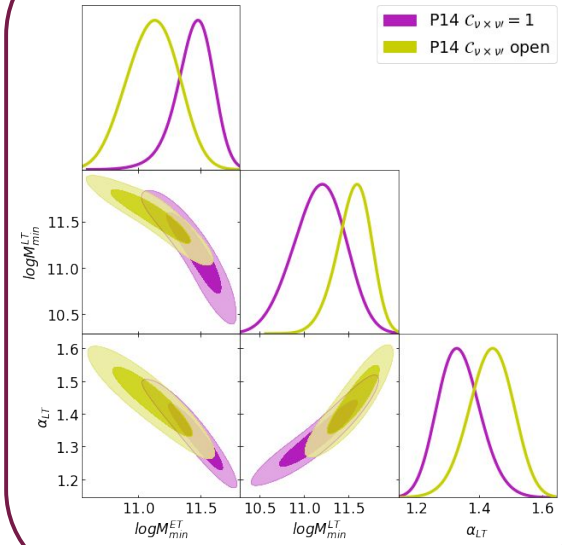

Zagatti et al. 2024

- $\alpha_{\rm ET}$ unconstrained

Planck data

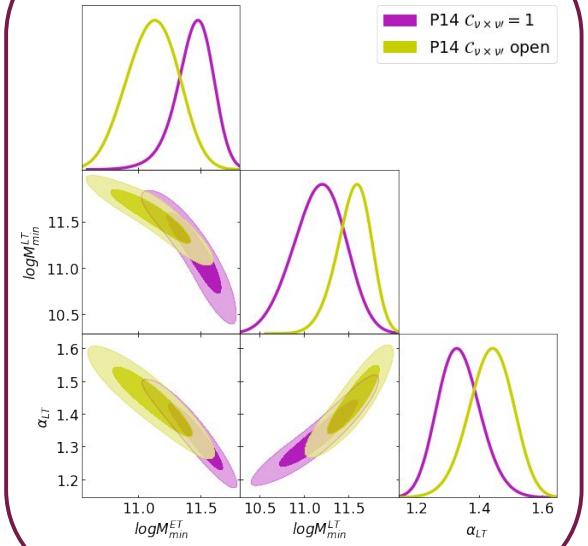

Zagatti et al. 2024

- $\alpha_{\rm ET}$ unconstrained

Planck-Lenz analysis

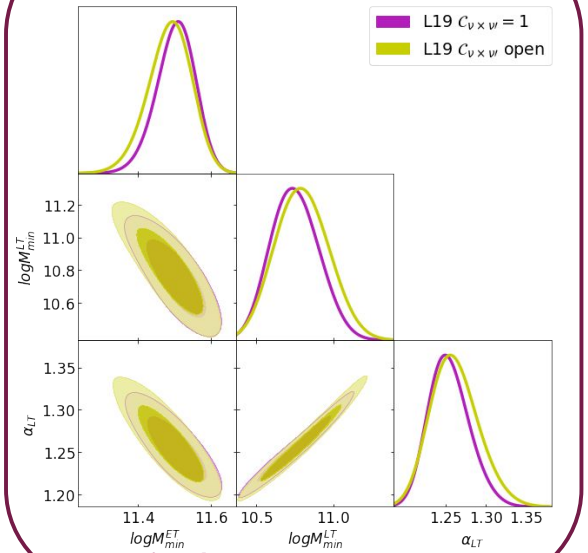

Zagatti et al. 2024

- Too high χ^2, only qualitative conclusions

Hint of possible dust contamination

Planck data

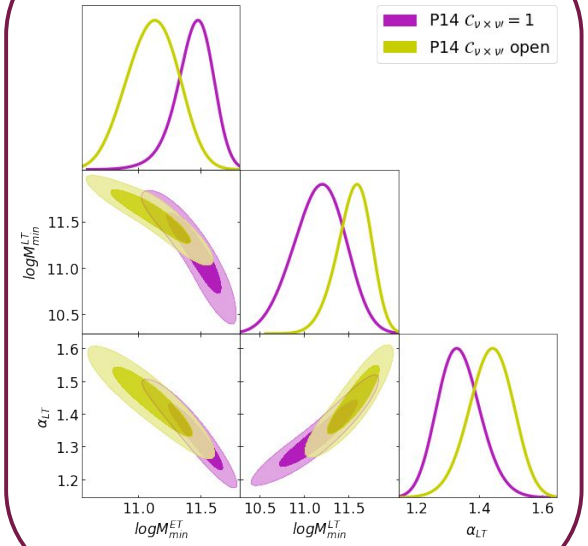

Zagatti et al. 2024

- $\alpha_{\rm ET}$ unconstrained

Planck-Lenz analysis

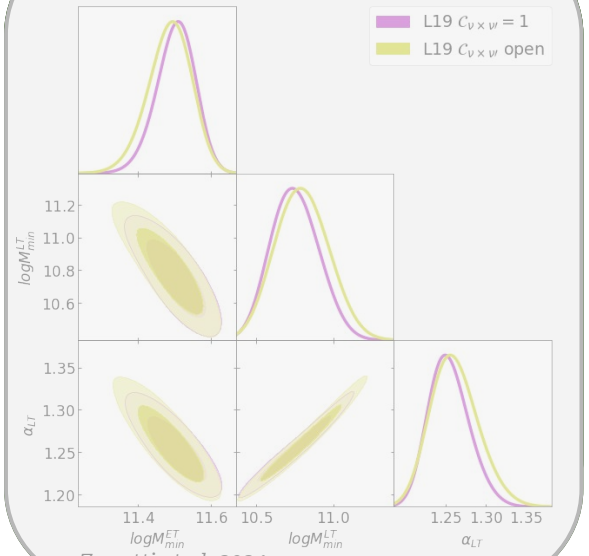

Zagatti et al. 2024

- Too high χ^2, only qualitative conclusions

Hint of possible dust contamination

Planck data

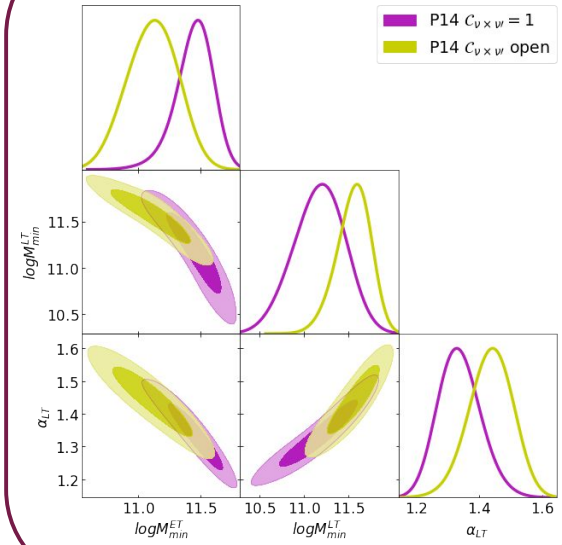

Zagatti et al. 2024

- $\alpha_{\rm ET}$ unconstrained

Planck-Lenz analysis

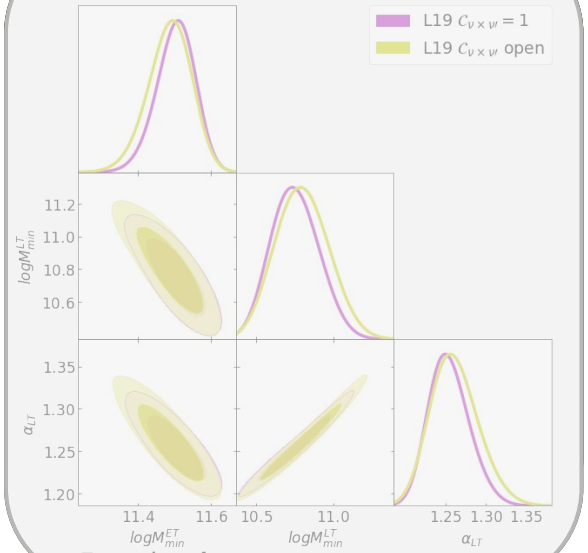

Zagatti et al. 2024

- Too high χ^2, only qualitative conclusions

Hint of possible dust contamination

Herschel-SPIRE data

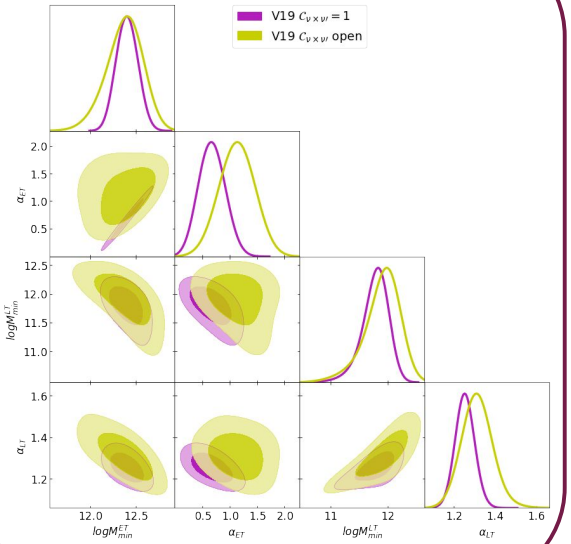

Zagatti et al. 2024

- $\alpha_{\rm ET}$ constrained

Planck data

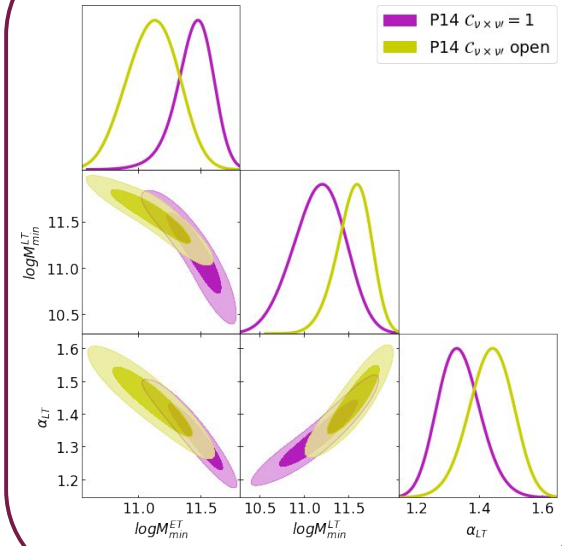

Zagatti et al. 2024

Parameter	$\mathcal{C}_{\nu_1\times\nu_2}=1$
$\log(M^{\rm ET}_{\rm min}/M_\odot h^{-1})$	$11.45^{+0.16}_{-0.13}$
$\log(M^{\rm LT}_{\rm min}/M_\odot h^{-1})$	$11.18^{+0.31}_{-0.27}$
$\alpha_{\rm LT}$	$1.337^{+0.063}_{-0.072}$

Parameter	$\mathcal{C}_{\nu_1\times\nu_2}=1$
$\log(M^{\rm ET}_{\rm min}/M_\odot h^{-1})$	12.40 ± 0.11
$\alpha_{\rm ET}$	0.67 ± 0.23
$\log(M^{\rm LT}_{\rm min}/M_\odot h^{-1})$	$11.79^{+0.25}_{-0.19}$
$\alpha_{\rm LT}$	1.253 ± 0.044

Herschel-SPIRE data

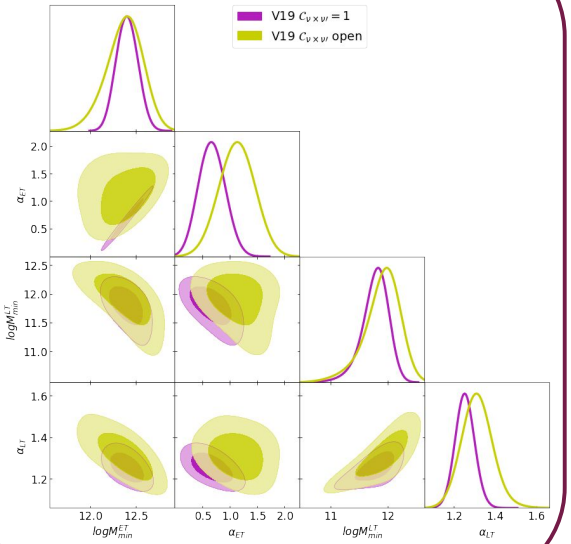

Zagatti et al. 2024

- $\alpha_{\rm ET}$ unconstrained
- $\alpha_{\rm ET}$ constrained

Planck data

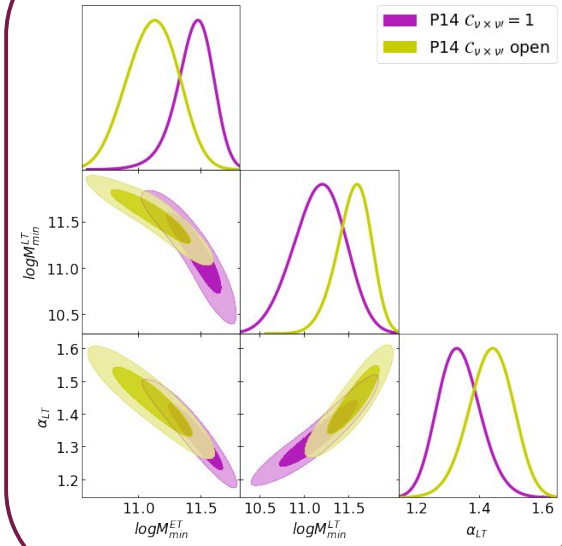

Zagatti et al. 2024

Parameter	$\mathcal{C}_{\nu_1\times\nu_2}=1$
$\log(M^{\rm ET}_{\rm min}/M_\odot h^{-1})$	$11.45^{+0.16}_{-0.13}$
$\log(M^{\rm LT}_{\rm min}/M_\odot h^{-1})$	$11.18^{+0.31}_{-0.27}$
$\alpha_{\rm LT}$	$1.337^{+0.063}_{-0.072}$

Parameter	$\mathcal{C}_{\nu_1\times\nu_2}=1$
$\log(M^{\rm ET}_{\rm min}/M_\odot h^{-1})$	12.40 ± 0.11
$\alpha_{\rm ET}$	0.67 ± 0.23
$\log(M^{\rm LT}_{\rm min}/M_\odot h^{-1})$	$11.79^{+0.25}_{-0.19}$
$\alpha_{\rm LT}$	1.253 ± 0.044

Herschel-SPIRE data

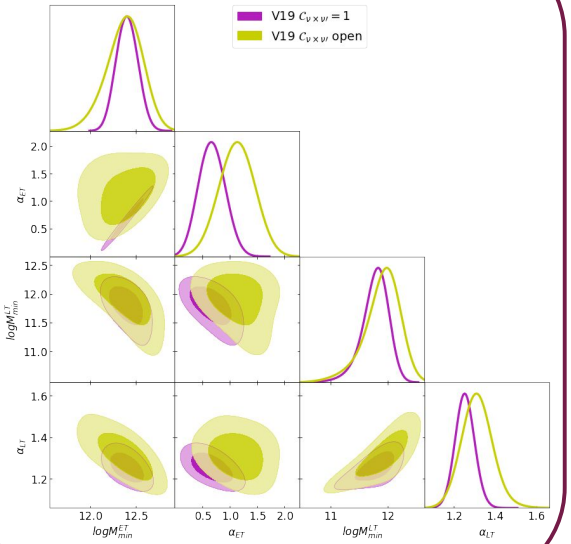

Zagatti et al. 2024

- $\alpha_{\rm ET}$ unconstrained
- $\alpha_{\rm ET}$ constrained

Planck and Herschel-SPIRE comparison

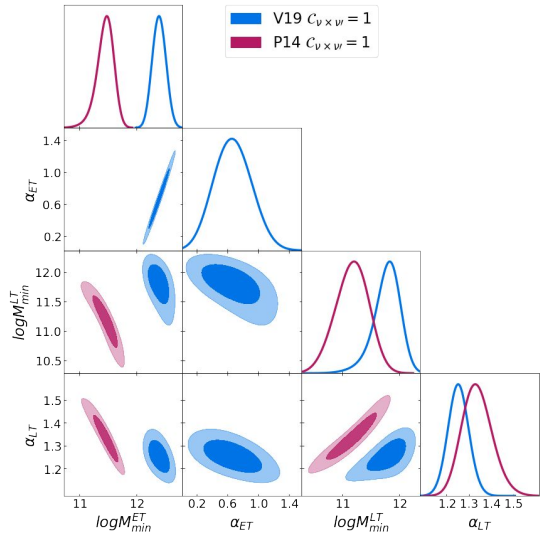

Zagatti et al. 2024

- *No unique model for all frequencies and angular scales*
- *No joint fit*
- *Issues with the datasets*
  Maniyar et al. (2018, 2021)

5σ tension between the best fit values of the minimum mass for ET galaxies.

All the attempts to alleviate the tension among the two datasets have failed.

Planck and Herschel-SPIRE comparison

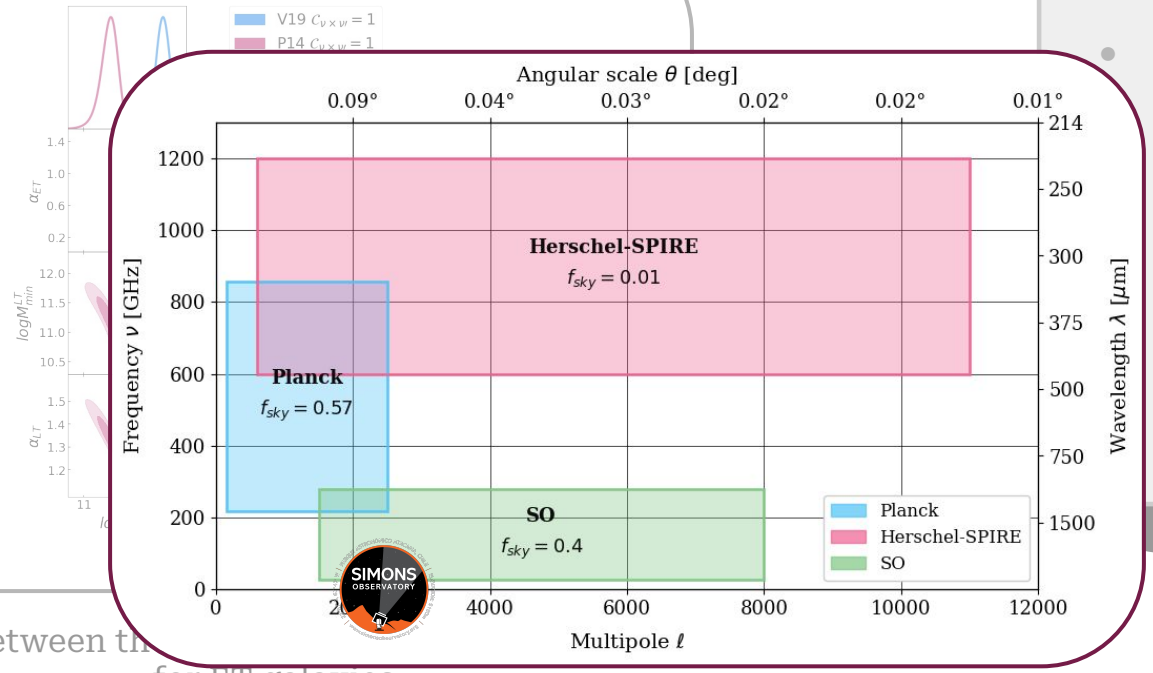

- *No unique model for all frequencies and angular scales*
- *No joint fit*
- *Issues with the datasets*
  Maniyar et al. (2018, 2021)

5σ tension between th
for ET galaxies.

All the attempts to alleviate the tension among the two datasets have failed.

Extragalactic Carbon-Monoxide (CO) → A forgotten signal in CMB analysis pipelines?

Maniyar+23
Kokron+24
Mehta+25

Extragalactic Carbon-Monoxide (CO)

Diatomic Molecule

Rotational transition
J→J−1

NO continuous spectrum

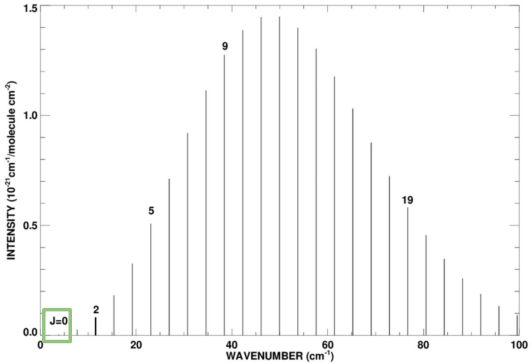

ν_{rest} ~ 115 GHz

→ A forgotten signal in CMB analysis pipelines?

Maniyar+23
Kokron+24
Mehta+25

Extragalactic Carbon-Monoxide (CO) → A forgotten signal in CMB analysis pipelines?

Maniyar+23
Kokron+24
Mehta+25

Diatomic Molecule

Rotational transition
J→J−1

NO continuous spectrum

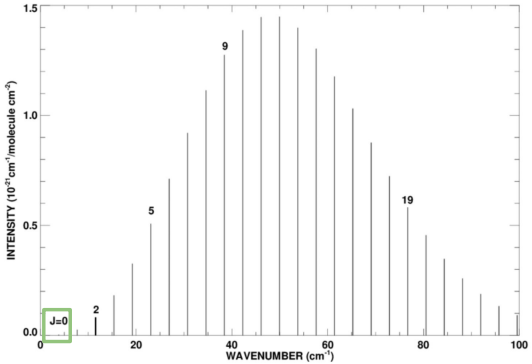

ν_{rest} ~ 115 GHz

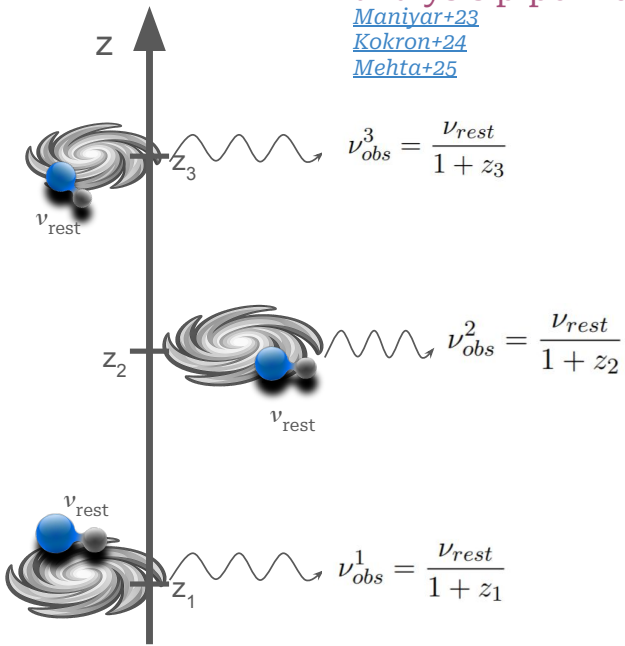

$$\nu^3_{obs} = \frac{\nu_{rest}}{1+z_3}$$

$$\nu^2_{obs} = \frac{\nu_{rest}}{1+z_2}$$

$$\nu^1_{obs} = \frac{\nu_{rest}}{1+z_1}$$

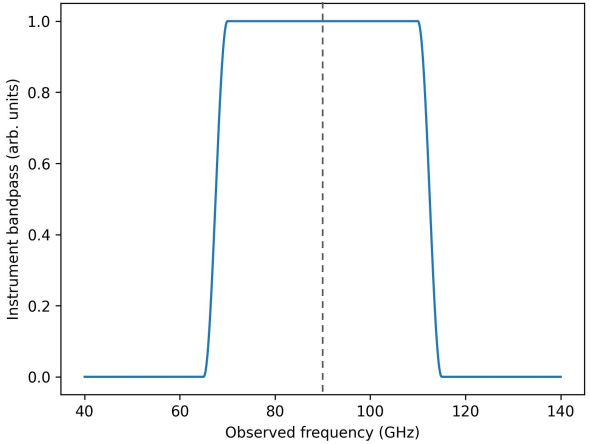

$$\Delta z_{CO(J\to J-1)} = z^{CO(J\to J-1)}_{max} - z^{CO(J\to J-1)}_{min}$$
$$= \frac{\nu^{CO(J\to J-1)}_{rest}}{\nu_{obs} - \frac{\Delta\nu}{2}} - \frac{\nu^{CO(J\to J-1)}_{rest}}{\nu_{obs} + \frac{\Delta\nu}{2}}$$

Extragalactic Carbon-Monoxide (CO)

Diatomic Molecule

Rotational transition
J→J−1

NO continuous spectrum

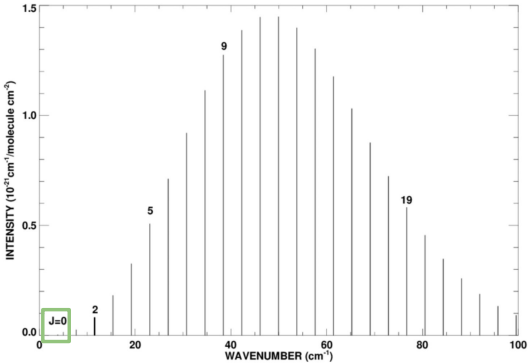

ν_{rest} ~ 115 GHz

→ A forgotten signal in CMB analysis pipelines?

[Maniyar+23](#)
[Kokron+24](#)
[Mehta+25](#)

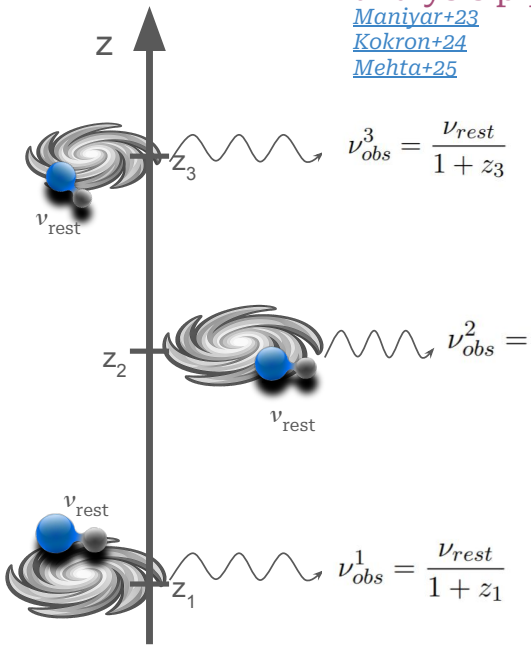

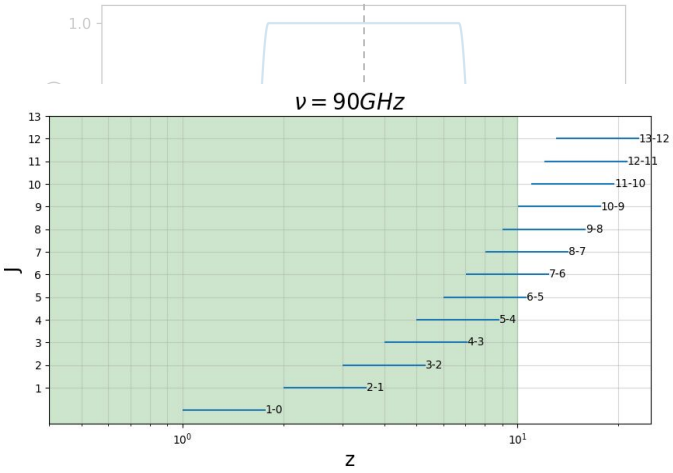

$$\Delta z_{CO(J\to J-1)} = z^{CO(J\to J-1)}_{max} - z^{CO(J\to J-1)}_{min}$$

$$CO(J\to J-1) \qquad CO(J\to J-1) \qquad \frac{\Delta\nu}{2}$$

Different CO transitions originating at different redshifts can be observed within the same CMB frequency band

Extragalactic Carbon-Monoxide (CO)

→ A forgotten signal in CMB analysis pipelines?

[Maniyar+23](#) [Kokron+24](#) [Mehta+25](#)

Diatomic Molecule

Rotational transition
J→J−1

NO continuous spectrum

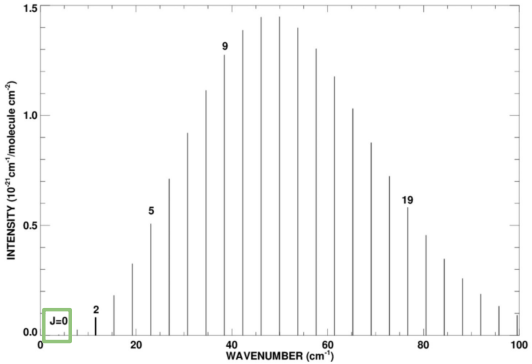

ν_{rest} ~ 115 GHz

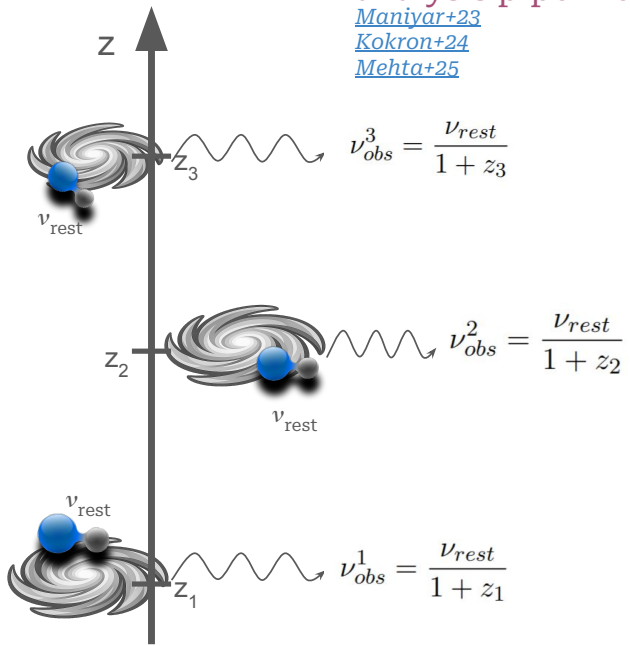

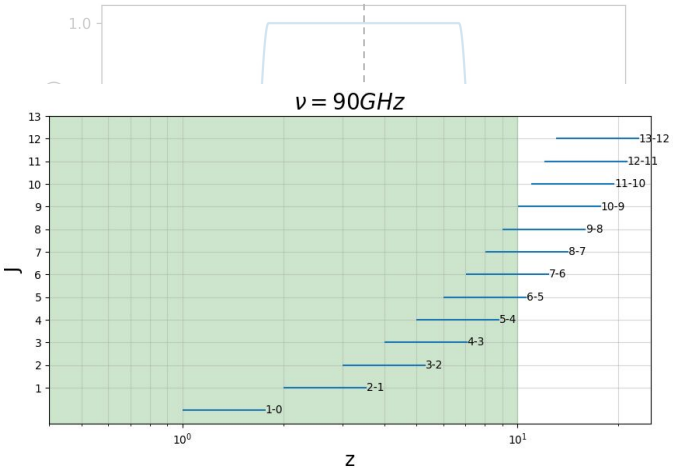

$$\Delta z_{CO(J\to J-1)} = z^{CO(J\to J-1)}_{max} - z^{CO(J\to J-1)}_{min}$$

$$\frac{\Delta\nu}{2}$$

Different CO transitions originating at different redshifts can be observed within the same CMB frequency band

Extragalactic CO as a continuous emission

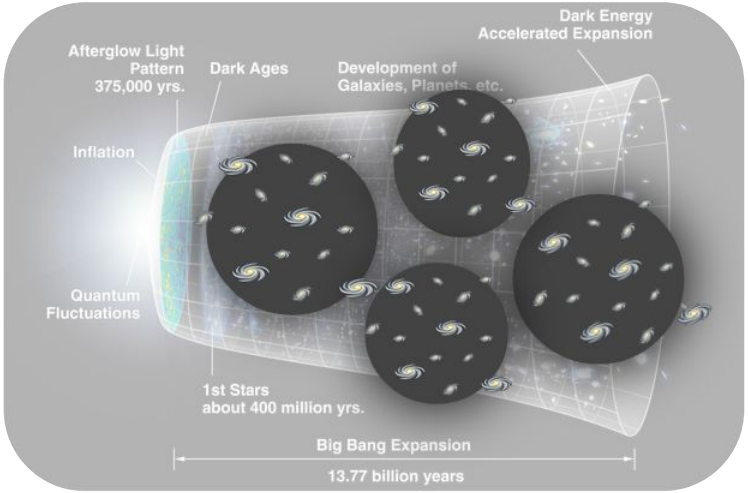
Dark Energy
Accelerated Expansion
Afterglow Light
Pattern
375,000 yrs.
Dark Ages
Development of
Galaxies, Planets, etc.
Inflation
Quantum
Fluctuations
1st Stars
about 400 million yrs.
Big Bang Expansion
13.77 billion years

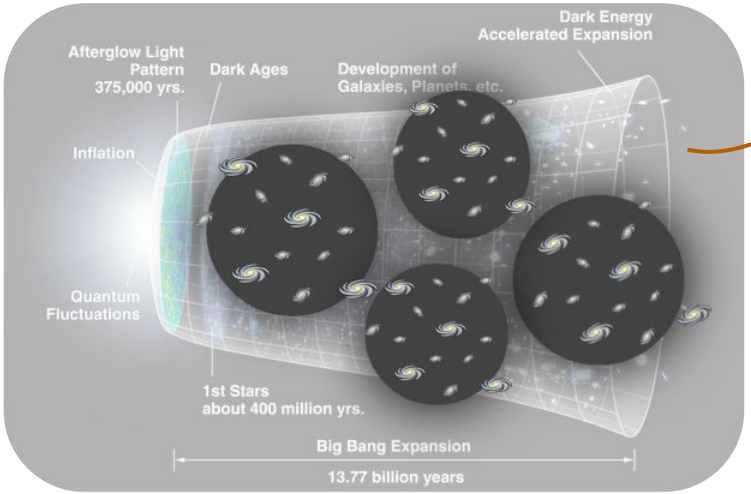
Afterglow Light Pattern 375,000 yrs.
Dark Ages
Development of Galaxies, Planets, etc.
Dark Energy Accelerated Expansion
Inflation
Quantum Fluctuations
1st Stars about 400 million yrs.
Big Bang Expansion
13.77 billion years

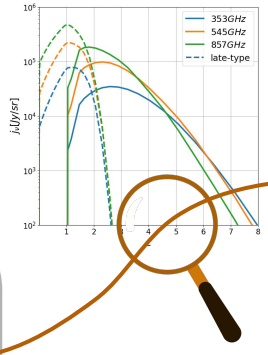
353GHz
545GHz
857GHz
late-type
[μJy/sr]
ℓ

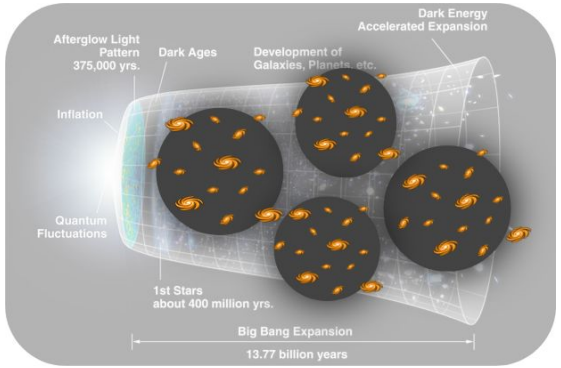
Afterglow Light Pattern 375,000 yrs.
Dark Ages
Development of Galaxies, Planets, etc.
Dark Energy Accelerated Expansion
Inflation
Quantum Fluctuations
1st Stars about 400 million yrs.
Big Bang Expansion
13.77 billion years

CIBxCIB

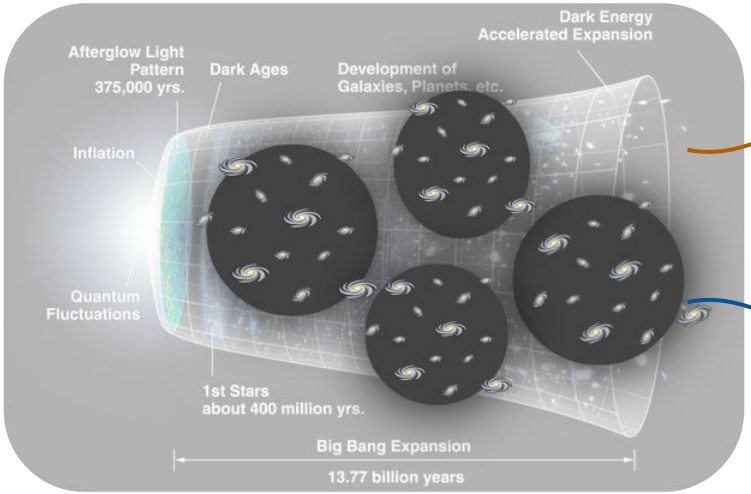

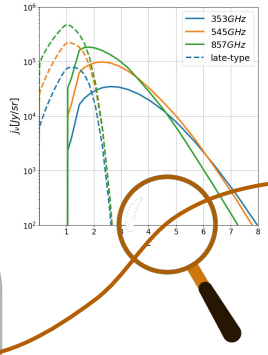

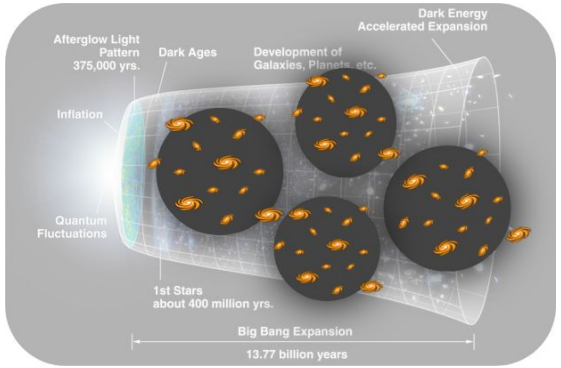

CIBxCIB

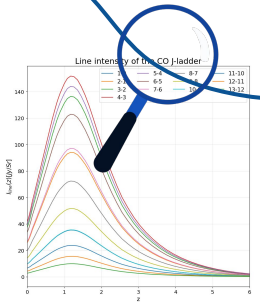

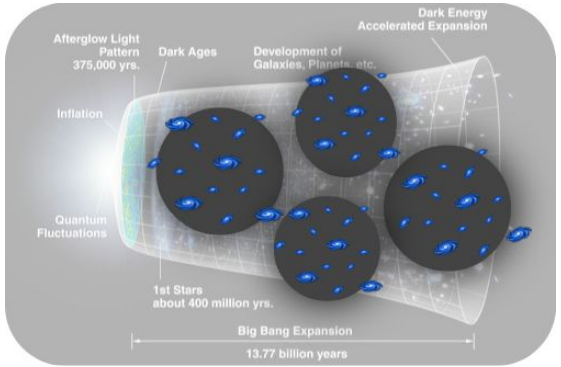

COxCO

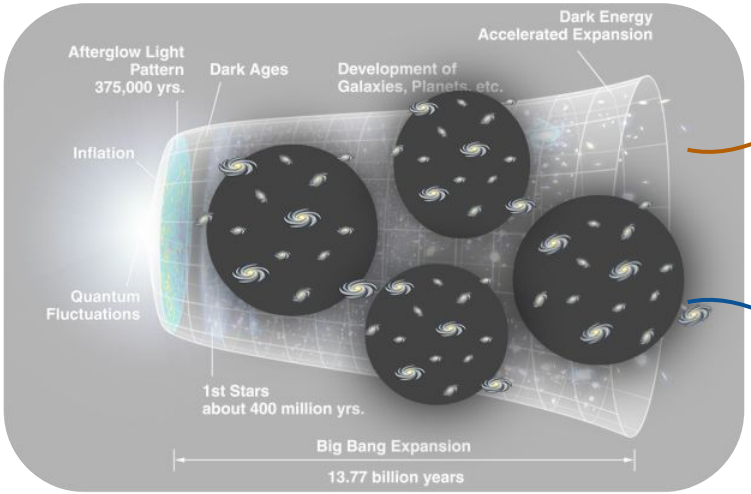

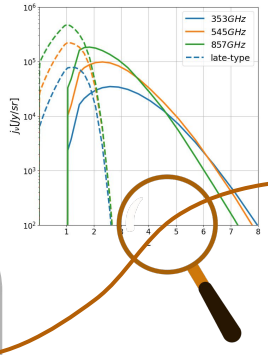

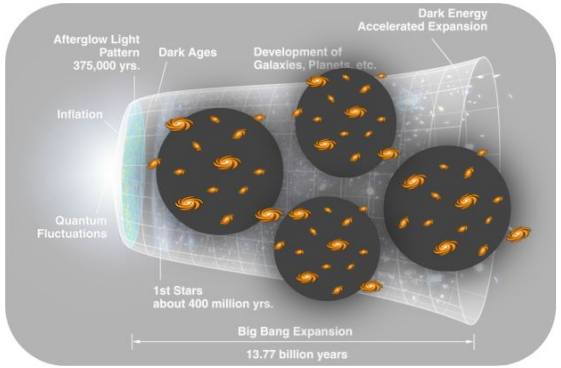

CIBxCIB

COxCIB

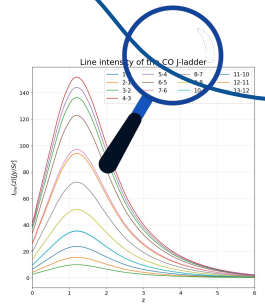

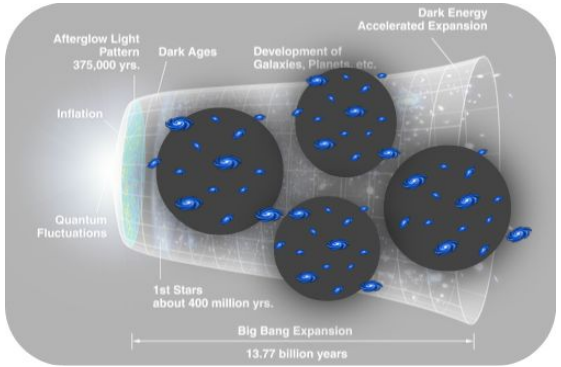

COxCO

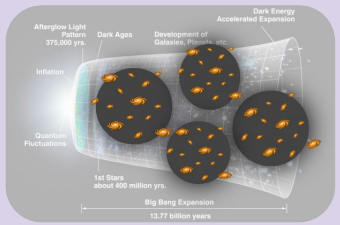

CIBxCIB

COxCIB

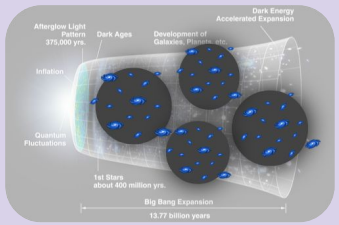

COxCO

Halo Model formalism employed to compute power spectra of **different tracers** and their **cross correlations**

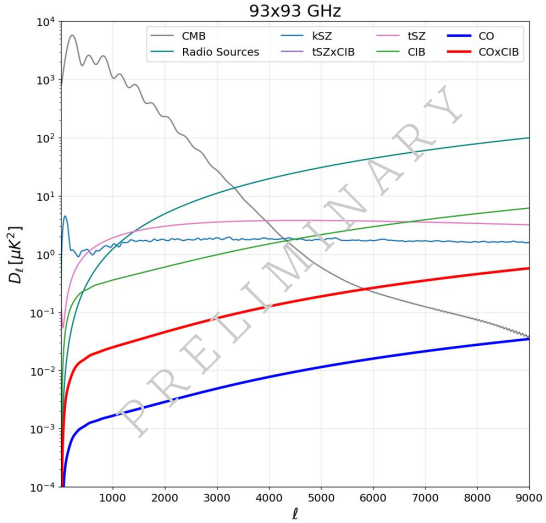

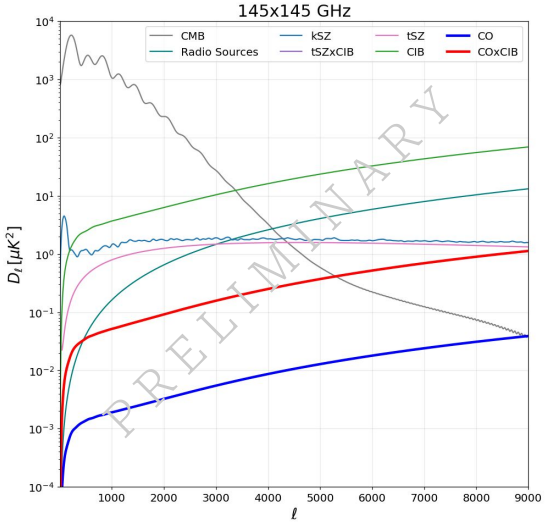

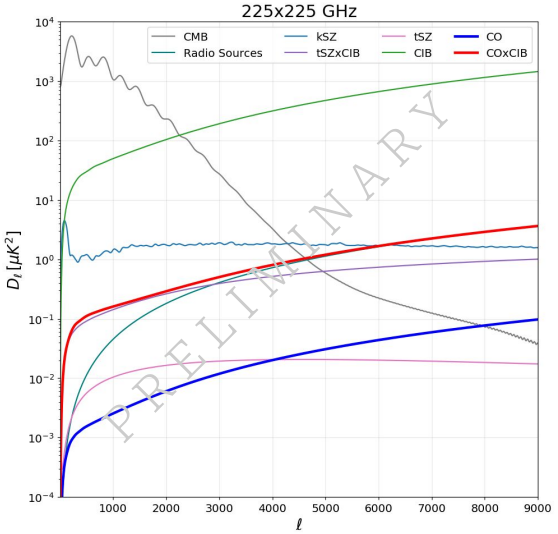

Zagatti et al. in preparation

CIBxCIB

COxCIB

COxCO

Halo Model formalism employed to compute power spectra of **different tracers** and their **cross correlations**

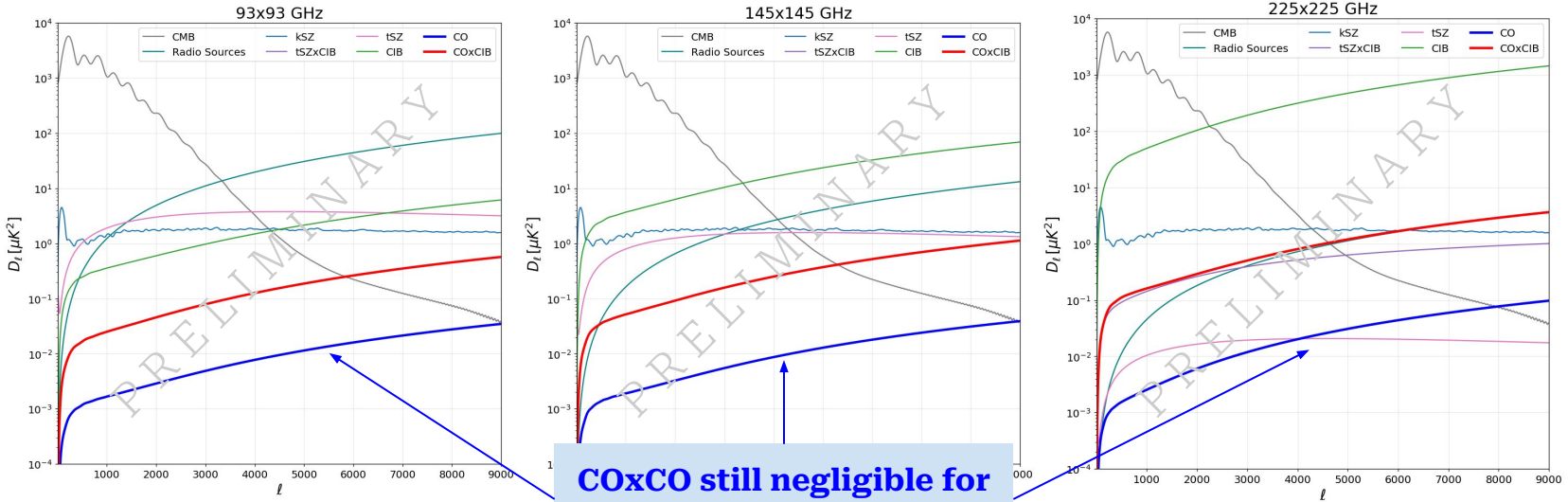

Zagatti et al. in preparation

COxCO still negligible for CMB frequency channels

CIBxCIB

COxCIB

COxCO

Halo Model formalism employed to compute power spectra of **different tracers** and their **cross correlations**

COxCIB comparable to other extragalactic signals included in CMB analyses

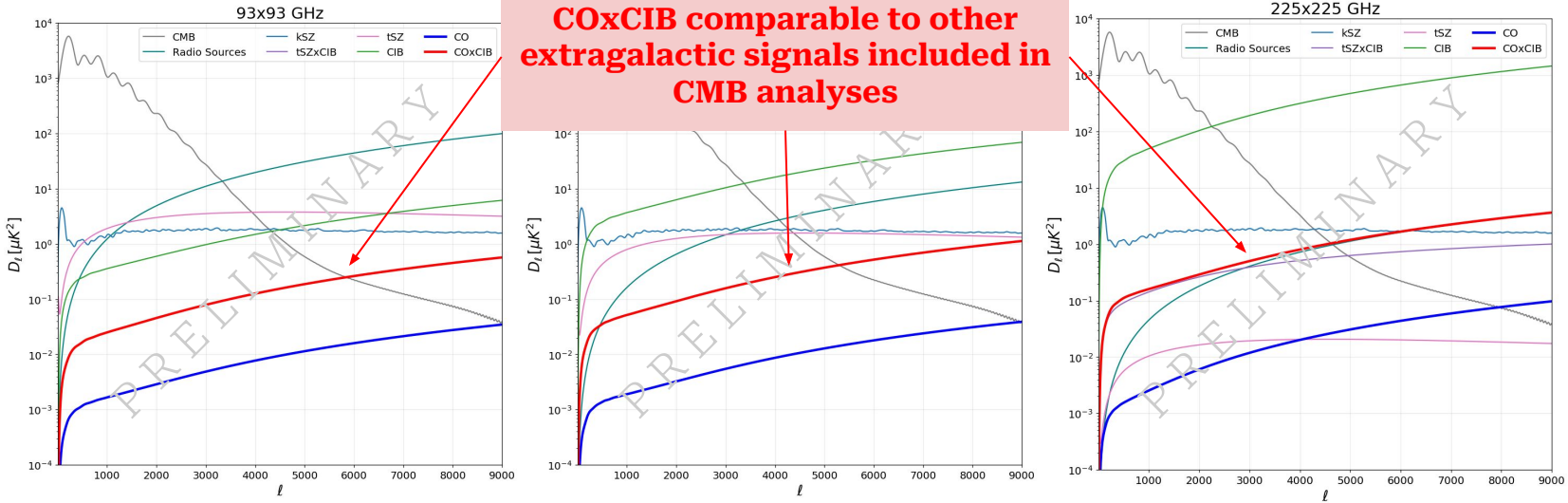

Zagatti et al. in preparation

Cosmic Infrared Background

- Implementation of a full shape **two galaxy population** description of the **CIB** based on a **Halo Model** framework
- **Improvement** with respect to available *single galaxy population* models
- Same dataset-related issues found by previous works

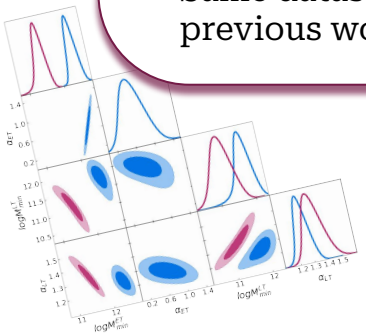

Extragalactic CO

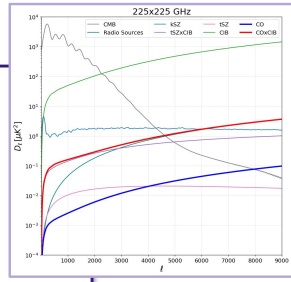

- Extension of the Halo Model to the evaluation of the extragalactic CO power spectrum
- Analytic model for **COxCO** and **COxCIB** power spectra

Need of a **physically motivated** and **comprehensive** model of foregrounds emission for forthcoming CMB experiments

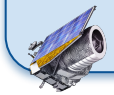

Backup Slides

$$P^{1h}_{uv}(k) = \int_0^\infty \hat{W}_u(m,k)\hat{W}_v(m,k)\frac{\mathrm{d}n}{\mathrm{d}m}\mathrm{d}m;$$

$$P^{2h}_{uv} = P^{lin}_{mm}(k)\prod_{n=u,v}\left[\int_o^\infty \hat{W}_n(m,k)b(m)\frac{\mathrm{d}n}{\mathrm{d}m}\mathrm{d}m\right].$$

- $$f(\sigma,z) = A(z)\left[\left(\frac{\sigma}{b(z)}\right)^{-a(z)} + 1\right]e^{-c(z)/\sigma^2}$$
- $\delta_h(m,z_1|M,V,z_0) = b(m,z_1)\delta,$
  $$b(m,z_1) = 1 - A\frac{\nu^a}{\nu^a + \delta_c^a} + B\nu^b + C\nu^c,$$
- $$\rho(r) = \frac{\rho_s}{r/r_s(1+r/r_s)^2}$$

$$P^{1h}_{\mathrm{ET}}(k) = \frac{1}{\left(\overline{n}^{\mathrm{ET}}_{\mathrm{gal}}\right)^2}\int_0^\infty \mathrm{d}m\frac{\mathrm{d}n}{\mathrm{d}m}[2N^{\mathrm{ET}}_{\mathrm{cent}}N^{\mathrm{ET}}_{\mathrm{sat}}u(m,k)+ \left(N^{\mathrm{ET}}_{\mathrm{sat}}\right)^2 u(k,m)^2],$$

$$P^{1h}_{\mathrm{LT}}(k) = \frac{1}{\left(\overline{n}^{\mathrm{LT}}_{\mathrm{gal}}\right)^2}\int_0^\infty \mathrm{d}m\frac{\mathrm{d}n}{\mathrm{d}m}[2N^{\mathrm{LT}}_{\mathrm{cent}}N^{\mathrm{LT}}_{\mathrm{sat}}u(m,k)+ \left(N^{\mathrm{LT}}_{\mathrm{sat}}\right)^2 u(k,m)^2],$$

$$P^{2h}_{\mathrm{ET}}(k) = P^{lin}_{mm}(k)\left[\int_0^\infty \mathrm{d}m\frac{\mathrm{d}n}{\mathrm{d}m}b(m)\frac{N^{\mathrm{ET}}_{\mathrm{gal}}}{\overline{n}^{\mathrm{ET}}_{\mathrm{gal}}}u(k,m)\right]^2,$$

$$P^{2h}_{\mathrm{LT}}(k) = P^{lin}_{mm}(k)\left[\int_0^\infty \mathrm{d}m\frac{\mathrm{d}n}{\mathrm{d}m}b(m)\frac{N^{\mathrm{LT}}_{\mathrm{gal}}}{\overline{n}^{\mathrm{LT}}_{\mathrm{gal}}}u(k,m)\right]^2.$$

$$P^{1h}_{\mathrm{mix}}(k) = \frac{1}{\overline{n}^{\mathrm{ET}}_{\mathrm{gal}}\overline{n}^{\mathrm{LT}}_{\mathrm{gal}}}\int_0^\infty \mathrm{d}m\frac{\mathrm{d}n}{\mathrm{d}m}[(N^{\mathrm{ET}}_{\mathrm{cent}}N^{\mathrm{LT}}_{\mathrm{sat}} + N^{\mathrm{ET}}_{\mathrm{sat}}N^{\mathrm{LT}}_{\mathrm{cent}})u+ N^{\mathrm{ET}}_{\mathrm{sat}}N^{\mathrm{LT}}_{\mathrm{sat}}u^2],$$

$$P^{2h}_{\mathrm{mix}}(k) = P^{lin}_{mm}\left[\int_0^\infty \mathrm{d}m\frac{\mathrm{d}n}{\mathrm{d}m}b(m)\frac{N^{\mathrm{ET}}_{\mathrm{gal}}}{\overline{n}^{\mathrm{ET}}_{\mathrm{gal}}}u\right]\times \left[\int_0^\infty \mathrm{d}m\frac{\mathrm{d}n}{\mathrm{d}m}b(m)\frac{N^{\mathrm{LT}}_{\mathrm{gal}}}{\overline{n}^{\mathrm{LT}}_{\mathrm{gal}}}u\right].$$

Non-linear galaxy power spectrum in a halo model framework

	X12	P11	C13
$\log(M^{\mathrm{ET}}_{\mathrm{min}}/M_\odot h^{-1})$	12.09 ± 0.06	$11.95 \pm 2.10-12.21 \pm 0.51$	12.00 ± 0.04
α_{ET}	1.81 ± 0.04	$1.02 \pm 0.87-1.30 \pm 1.16$	1.55 ± 0.05
$\log(M^{\mathrm{LT}}_{\mathrm{min}}/M_\odot h^{-1})$	$\equiv 10.85$	-	10.85 ± 0.06
α_{LT}	$\equiv 1$	-	$\equiv 1$

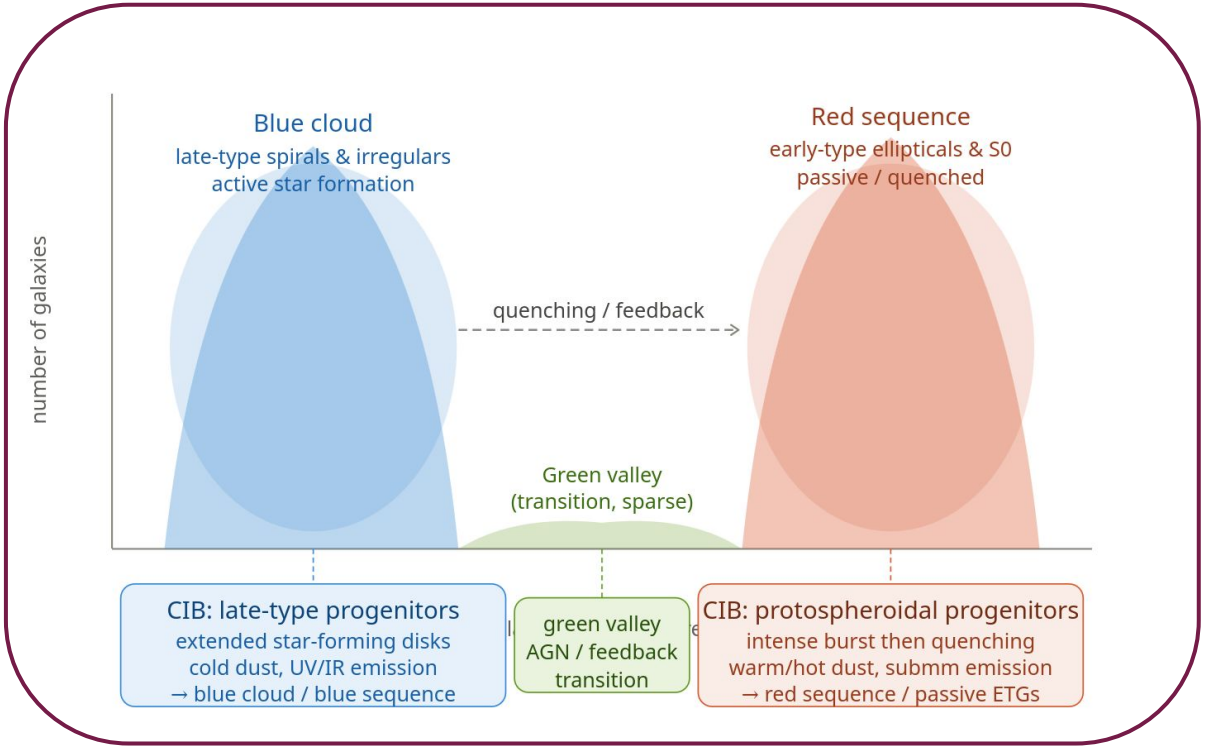

Less massive DM haloes, which more likely merge with other low mass DM haloes

More massive and more static DM haloes

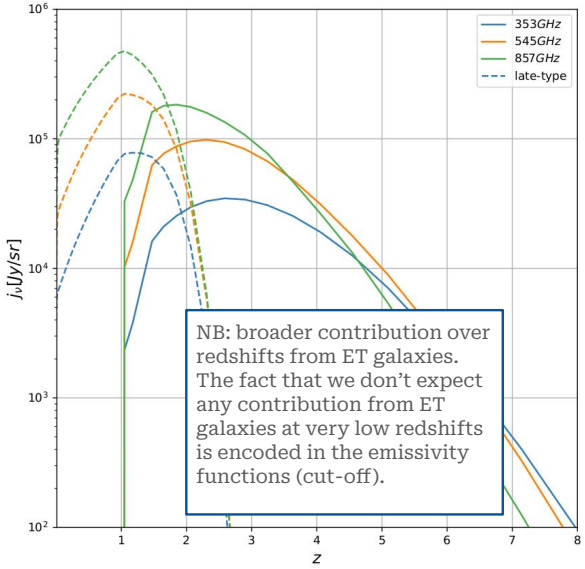

$$j_\nu(z) = \int_0^{S_\nu^{lim}} \frac{d^3N(S_\nu,z)}{dS_\nu dz d\Omega} S_\nu dS_\nu.$$

$$\frac{d^3N(S_\nu,z)}{dS_\nu dz d\Omega} = \frac{\Phi(\log L_{\nu'},z)}{L_{\nu'} \ln 10} \frac{dL_{\nu'}}{dS_\nu} \frac{d^2V}{dz d\Omega},$$

$$S_\nu = \frac{(1+z)L_{\nu'}}{4\pi D_L^2(z)},$$

Surface density of sources per unit flux density and redshift interval

flux density

$\Phi(\log L_{\nu'},z)$ LF

The luminosity function for ET galaxies is a convolution of the **halo formation rate** (obtained as the time derivative of the hmf) and the **galaxy luminosity distribution** (log-normal distribution).

$$\frac{dn}{dt_{vir}} = dn \frac{d\ln(\nu f(\nu))}{dt_{vir}}.$$

$$P(\log L|\log\bar{L})d\log L = \frac{\exp\{-\log^2(L/\bar{L})/2\sigma^2\}}{\sqrt{2\pi\sigma^2}} d\log L,$$

$$\Phi(\log L,z) = \int_{M_{vir}^{min}}^{M_{vir}^{max}} dM_{vir} \int_{z_{vir}^{min}}^{z_{vir}^{max}} dz_{vir} \left|\frac{dt_{vir}}{dz_{vir}}\right| \frac{dn}{dt_{vir}} P(\log L,z).$$

Required an empirical parameterization for the luminosity function of LT galaxies. (Cai et al. 2013)

$$\Phi(\log L_{IR},z)d\log L_{IR} = \Phi^* \left(\frac{L_{IR}}{L^*}\right)^{1-\alpha} \exp\left\{-\frac{\log^2(1+L_{IR}/L^*)}{2\sigma^2}\right\} d\log L_{IR},$$

$$L_\nu = \nu f(\nu) L_{bol}.$$

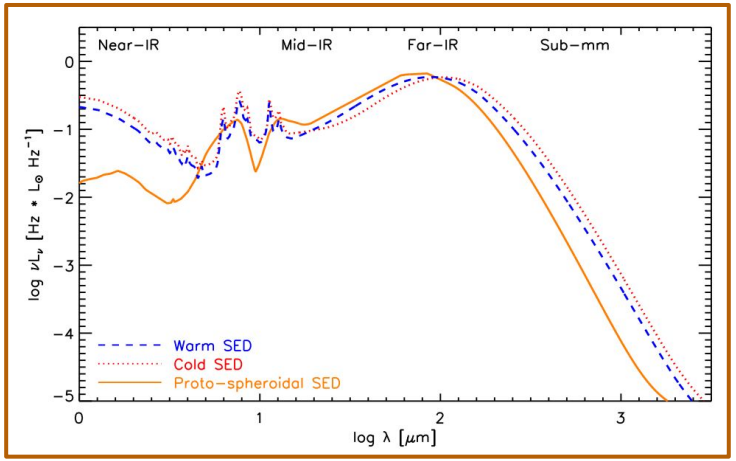

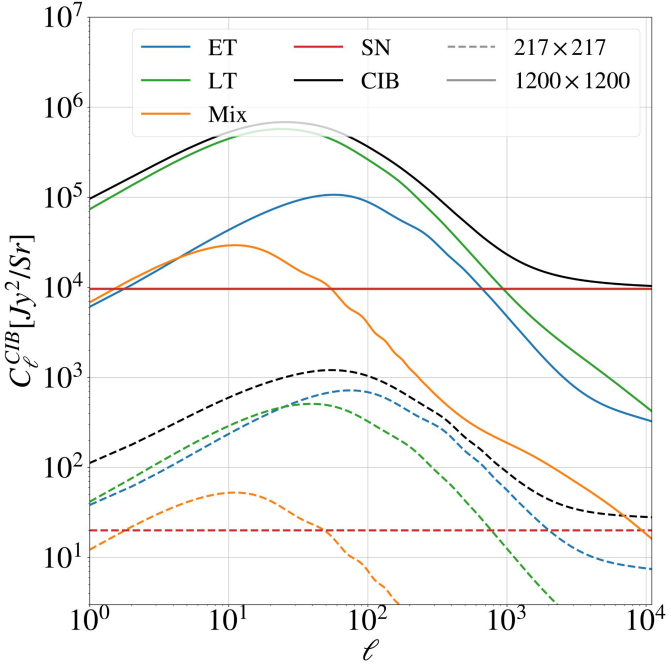

ET

clustering

Dataset	**Total area** (deg^2)	**Frequency channels** (GHz)	**Multipole range**	**Binning scheme**	**Color Correction**
P14	2240	217, 353, 545, 857	150-2500	Logarithmic	1.119, 1.097, 1.068, 0.995
L19	2240	353, 545, 857	75-2500	Linear	1.097, 1.068, 0.995
V19	90	600, 857, 1200	600-11000	Linear and logarithmic	0.9988, 0.9929, 0.9957

ET + LT

shot noise

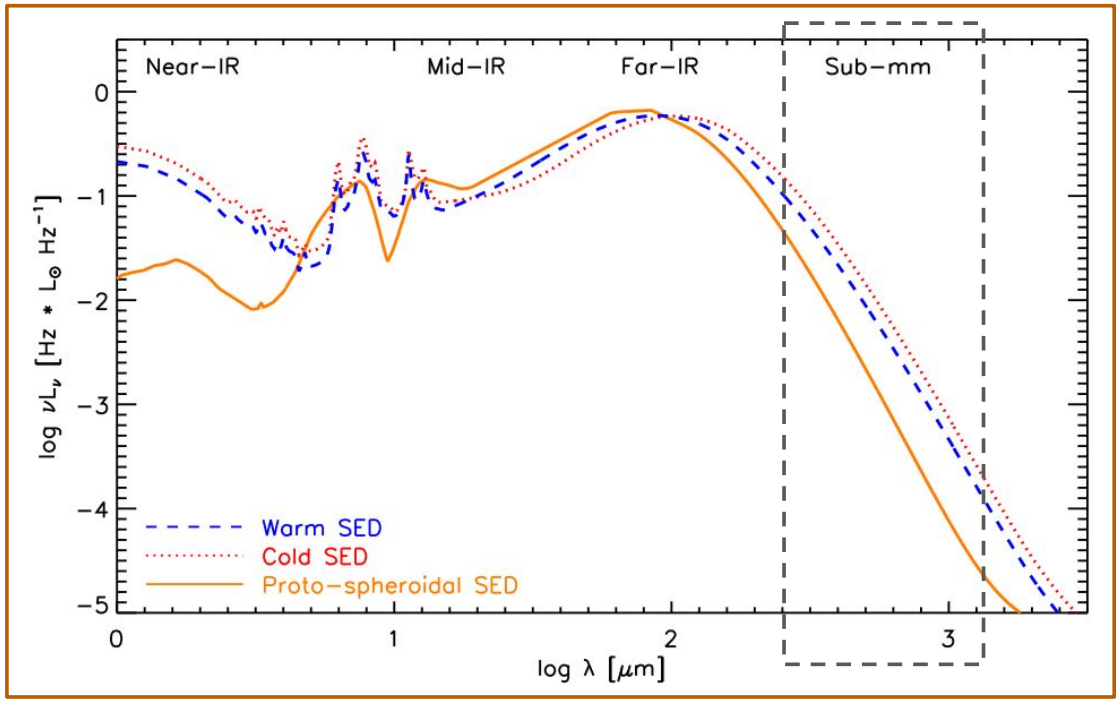

can start resolving the LT population individually

favours detecting the *integrated* CIB from rare, bright, high-z starbursts (ET progenitors) rather than resolving individual faint LT galaxies

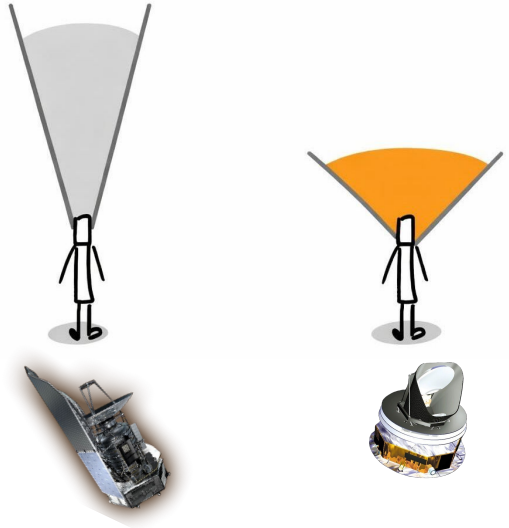

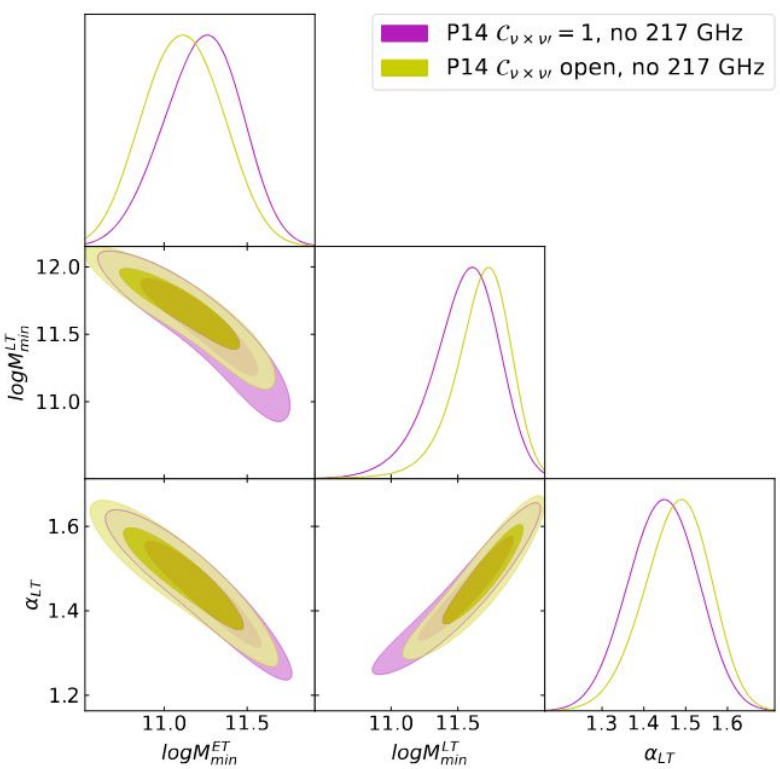

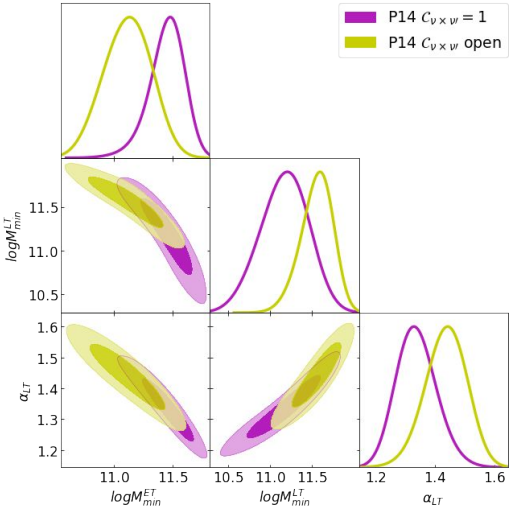

The exclusion of the 217GHz frequency channel makes the results of the fits more stable among the two scenarios.

Smaller shift in the 2D posterior distributions. To understand this we need to look at the full parameter space explored by the fit. We find a tension in the two scenarios for the value of the shot noise level of the 217 GHz frequency channel. Specifically, we obtain a value for the shot noise level which is higher in the case with free correlations than in the case with fixed correlations. We also see that the correlation coefficients involving the 217 GHz frequency channel are significantly lower than unity. We explain this behavior by noting the degeneracy between the shot noise level and the correlation coefficients at 217 GHz, which P14 data are not able to break. Specifically, they are anti-correlated, meaning that a shift of the shot noise level toward a lower value, closer to the one obtained in the first scenario, leads to higher values of the corr coeff.

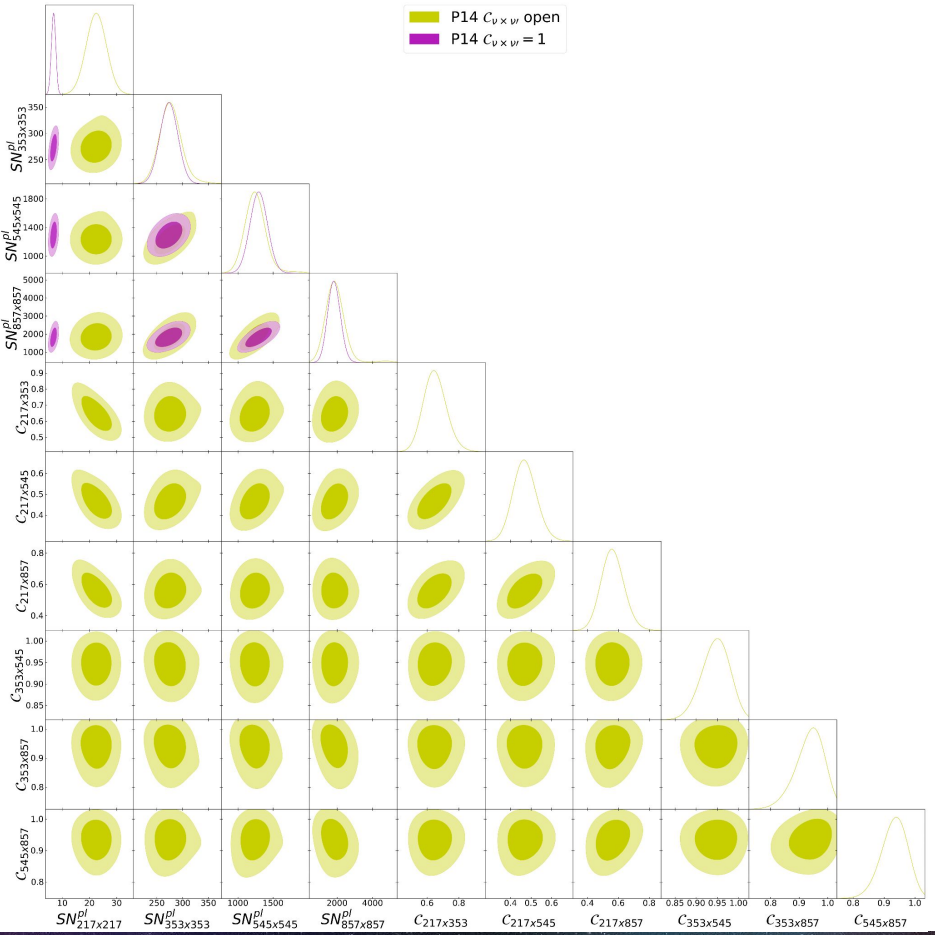

Parameter	Prior	Results $C_{\nu_1\times\nu_2}=1$	Results $C_{\nu_1\times\nu_2}$ open
$\log(M^{\rm ET}_{\rm min}/M_\odot h^{-1})$	[10.7,12.8]	$11.45^{+0.16}_{-0.13}$	11.12 ± 0.19
$\log(M^{\rm LT}_{\rm min}/M_\odot h^{-1})$	[10.5,12.8]	$11.18^{+0.31}_{-0.27}$	$11.56^{+0.21}_{-0.17}$
$\alpha_{\rm LT}$	[0.2,3.5]	$1.337^{+0.063}_{-0.072}$	$1.436^{+0.075}_{-0.067}$
$\rm SN_{217}$	[0,50]	6.72 ± 0.76	22 ± 4
$\rm SN_{353}$	[50,500]	273 ± 16	276 ± 20
$\rm SN_{545}$	[400,4000]	1296 ± 120	1247 ± 100
$\rm SN_{857}$	[200,8000]	1827 ± 300	1899^{+400}_{-600}
$f^{353}_{\rm cal}$	1 ± 0.0156	0.999 ± 0.014	1.010 ± 0.015
$f^{545}_{\rm cal}$	1 ± 0.122	1.096 ± 0.032	1.094 ± 0.032
$f^{857}_{\rm cal}$	1 ± 0.128	1.289 ± 0.076	1.200 ± 0.072
$C_{217\times353}$	[-1, 1]	-	$0.648^{+0.068}_{-0.075}$
$C_{217\times545}$	[-1, 1]	-	0.469 ± 0.054
$C_{217\times857}$	[-1, 1]	-	0.562 ± 0.070
$C_{353\times545}$	[-1, 1]	-	$0.946^{+0.035}_{-0.031}$
$C_{353\times857}$	[-1, 1]	-	$0.937^{+0.056}_{-0.042}$
$C_{545\times857}$	[-1, 1]	-	$0.934^{+0.046}_{-0.039}$

$$C^{SN}_{\ell,\nu\times\nu'} = \mathcal{C}_{\nu\times\nu'}\sqrt{SN_\nu \times SN_{\nu'}}$$

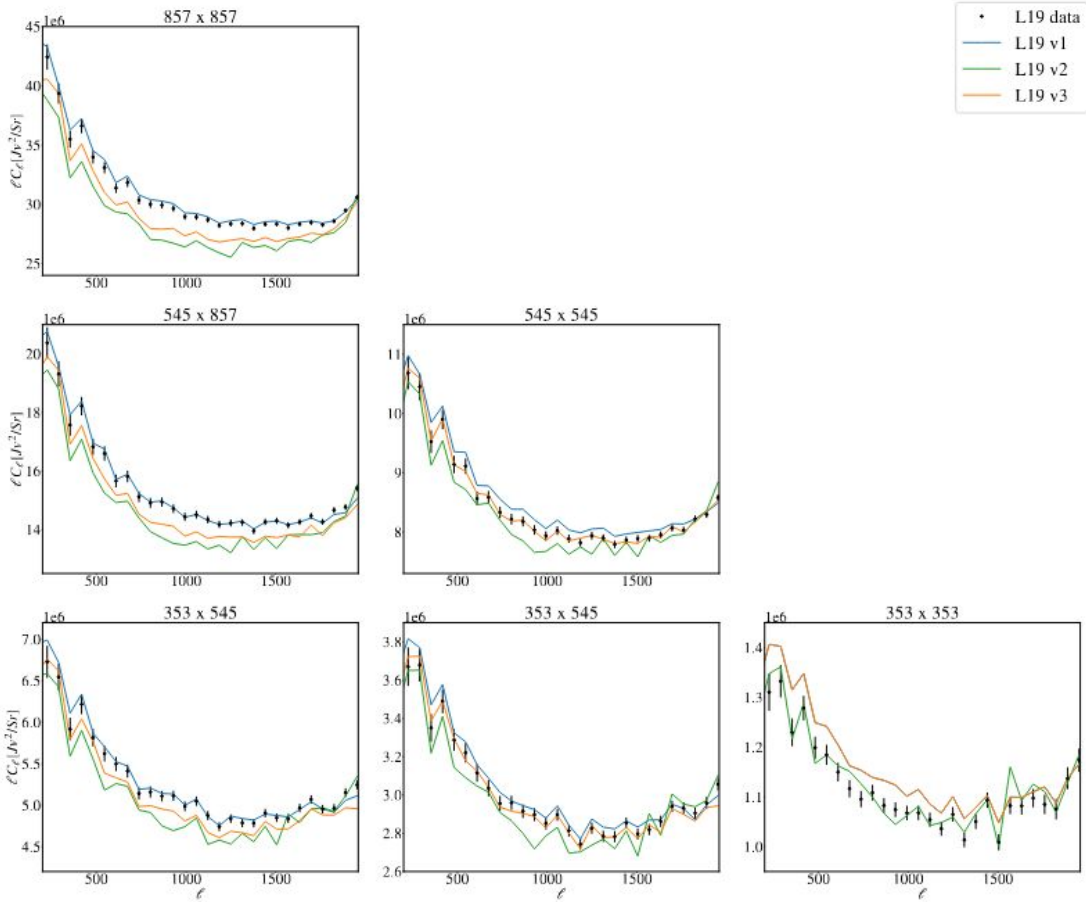

Three different datasets obtained after a re-analysis of the maps.

- The first version of the data set was obtained applying the same neutral hydrogen column density (N_{HI}) threshold of 2.5×10^{20} cm^{-2} across all three frequency channels (blue curve).
- The second data set applied a lower N_{HI} threshold of 1.5×10^{20} cm^{-2} across all channels to explore the impact of dust and in particular of dust residuals in the analysis (green curve).
- The third data set has been obtained following the prescription of L19 and imposing a different threshold for each frequency channel. Specifically we set $N_{HI} = 2.5 \times 10^{20}$ cm^{-2} , 2.0×10^{20} cm^{-2} and 1.8×10^{20} cm^{-2} for 353, 545 and 857 GHz respectively (orange curve).

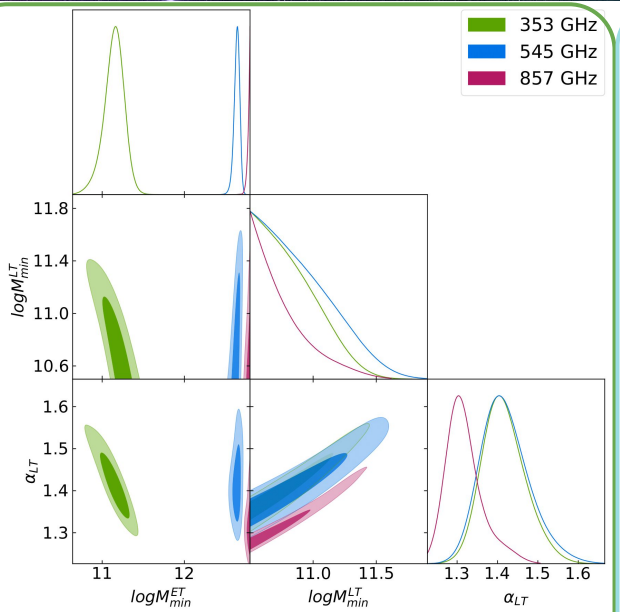

the two higher frequency channels result in much higher best-fit values for the Mmin of ET galaxies. Recalling that this clustering parameter acts as a re-scaling of the power spectrum, the high values could possibly be hinting at an excess of power coming from dust residuals.

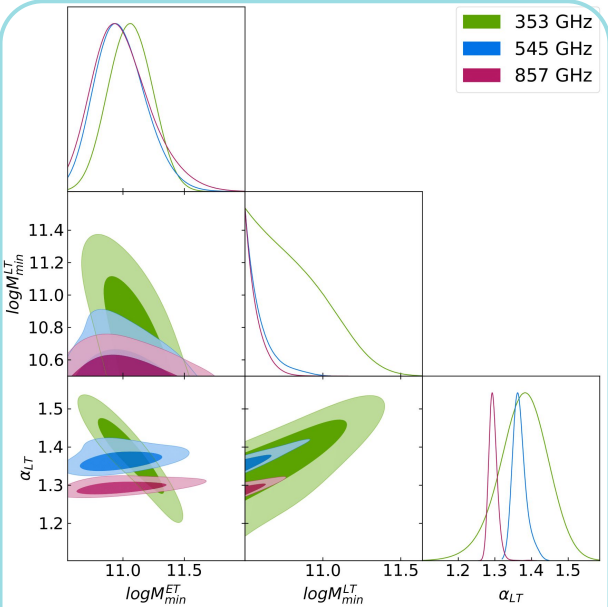

more aggressive mask, so smaller contamination. The behavior of the posterior distributions of the clustering parameters changes significantly. There is no tension between the minimum masses of ET galaxies, supporting the hypothesis of a ***dust residual***.

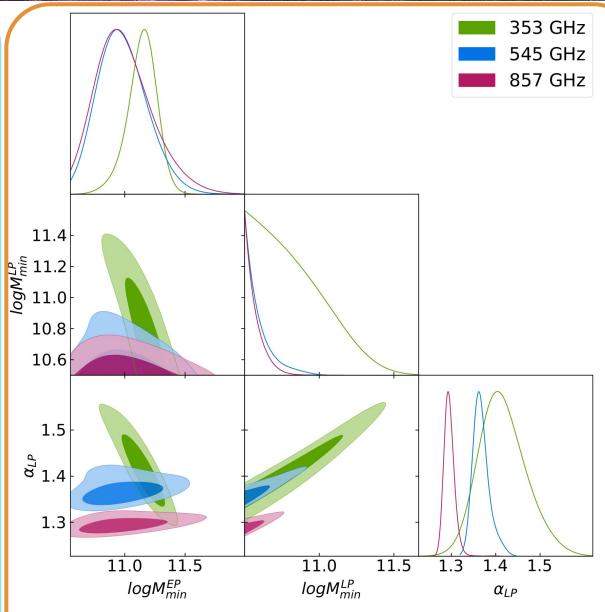

different thresholds for the three frequency channels, showed no significant differences from the second data set, except for the 353 GHz frequency channel which provided more constraining power due to more data retained.

P14 model vs data

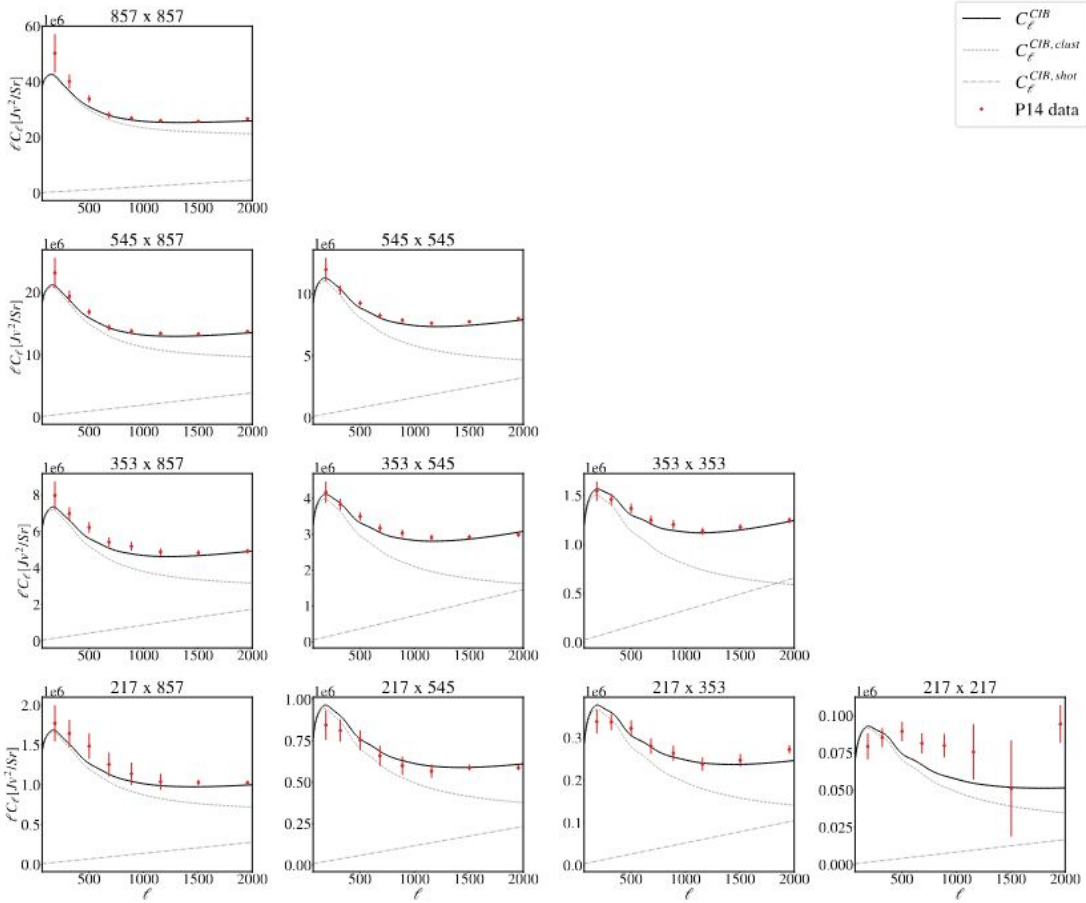

L19 model vs data

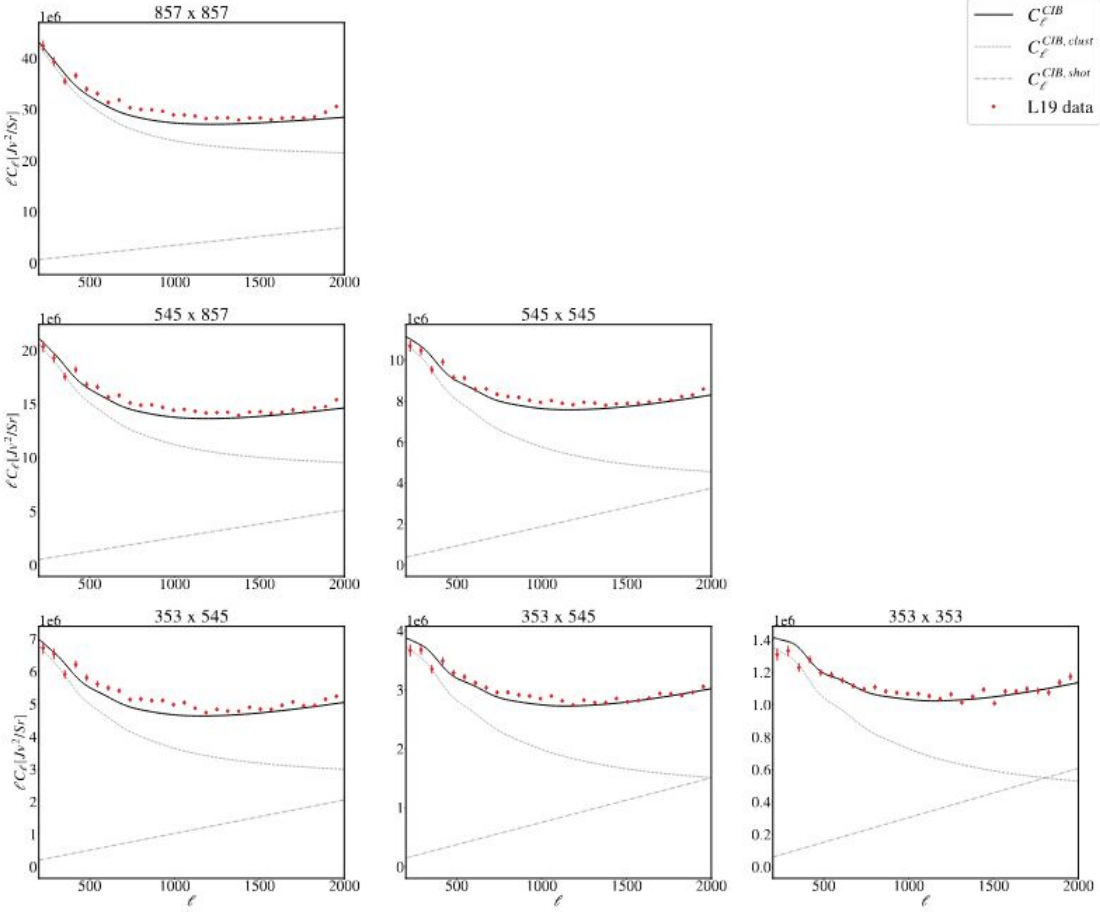

Model-Data comparison

$$\hat{C}^{model}_{\ell,\nu\times\nu'} = \underbrace{\mathcal{A}_{\nu\times\nu'} \times cc_{\nu} \times cc_{\nu'}}_{\text{Instrumental response}} \times C^{model}_{\ell,\nu\times\nu'}$$

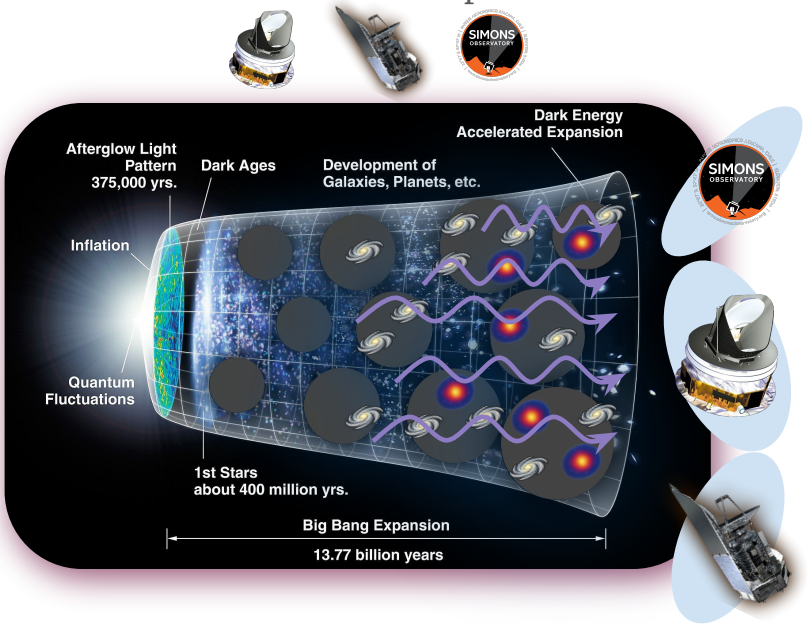

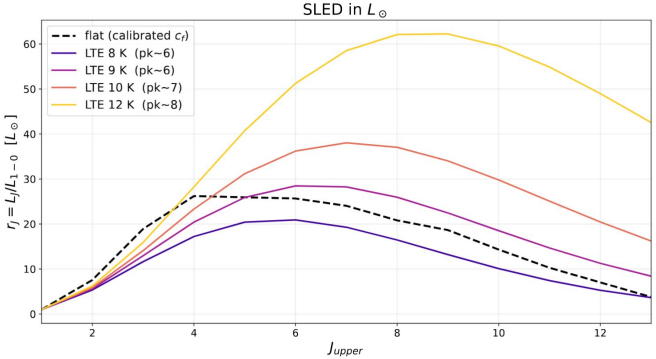
SLED in $L_\odot$
flat (calibrated c_ℓ)
LTE 8 K (pk~6)
LTE 9 K (pk~6)
LTE 10 K (pk~7)
LTE 12 K (pk~8)
$r_j = L_j/L_{1-0}$ [$L_\odot$]
J_{upper}

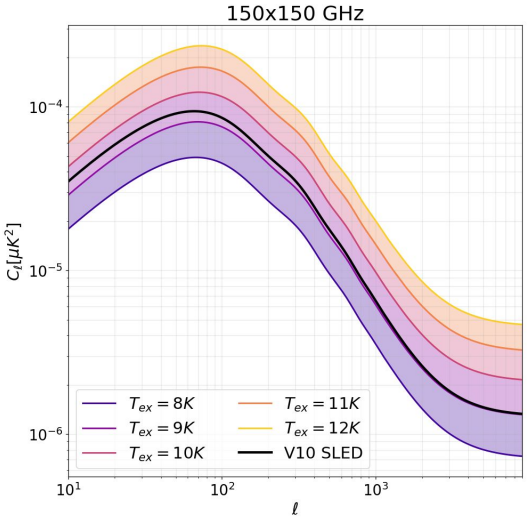
150x150 GHz
$C_\ell[\mu K^2]$
ℓ
$T_{ex} = 8K$
$T_{ex} = 9K$
$T_{ex} = 10K$
$T_{ex} = 11K$
$T_{ex} = 12K$
V10 SLED

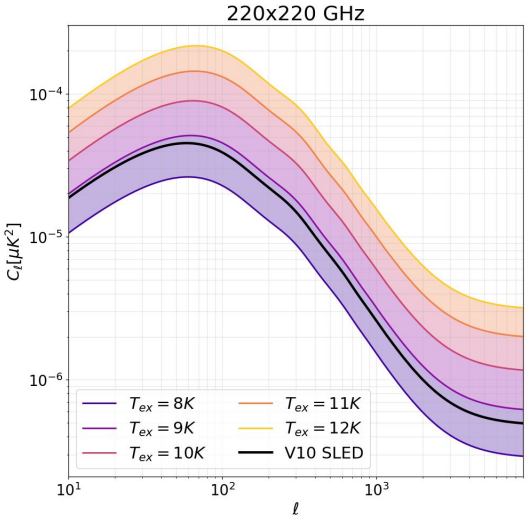
220x220 GHz
$C_\ell[\mu K^2]$
ℓ
$T_{ex} = 8K$
$T_{ex} = 9K$
$T_{ex} = 10K$
$T_{ex} = 11K$
$T_{ex} = 12K$
V10 SLED

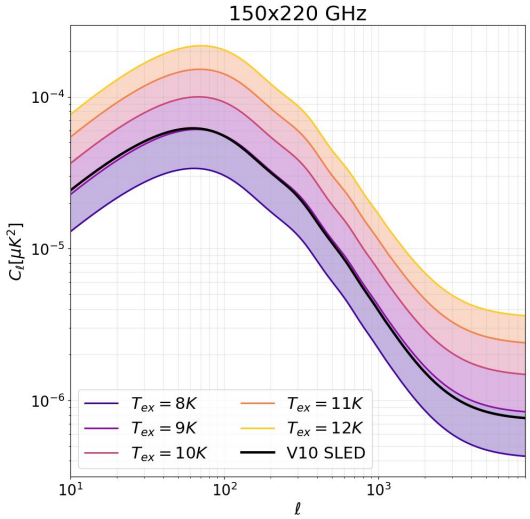
150x220 GHz
$C_\ell[\mu K^2]$
ℓ
$T_{ex} = 8K$
$T_{ex} = 9K$
$T_{ex} = 10K$
$T_{ex} = 11K$
$T_{ex} = 12K$
V10 SLED

COxCO

$$C_{\ell,\nu\times\nu'}^{CO(J)\times CO(J')} = \int \frac{d\chi}{dz}\frac{dz}{\chi^2}\xi_\nu^J(z)\xi_{\nu'}^{J'}(z)\left(P_{CO(J)\times CO(J')}^{tot}\right)$$

- $\xi_\nu(z) = \frac{c}{4\pi}\frac{1}{H(z)\Delta\nu(1+z)^2}\bar{j}\mathcal{R}_{\rm chan}(\nu_{\rm rest})$ emission/geometric kernel
  - $\bar{j}_J(z) \equiv \int dm \frac{dn}{dm}\left[\langle L_c\rangle + \langle L_s\rangle\right]$ mean emissivity
    - $L_{CO,c} = \langle N_c(m,z)\rangle\langle \ell_c\rangle$ central CO luminosity
    - $L_{CO,s} = \langle N_s(m,z)\rangle\langle \ell_s\rangle$ satellite CO luminosity
- $P_{CO\times CO} = P_{CO\times CO}^{1h} + P_{CO\times CO}^{2h} + P_{CO\times CO}^{shot}$ COxCO power spectrum
  - $P_{CO(J)\times CO(J')}^{1h} = \frac{1}{\bar{j}_J\bar{j}_{J'}}\int dm\frac{dn}{dm}\left[N_cN_s\left(\langle\ell_c^J\rangle\langle\ell_s^{J'}\rangle + \langle\ell_s^J\rangle\langle\ell_c^{J'}\rangle\right)\tilde{u}_{gal} + N_s(N_s-1)\langle\ell_s^J\rangle\langle\ell_s^{J'}\rangle\tilde{u}_{gal}^2\right]$; ⟶ 1h term
  - $P_{CO(J)\times CO(J')}^{2h} = P_{mm}^{lin}(k)\left[\frac{1}{\bar{j}_J}\int dm\frac{dn}{dm}b(m)\left(N_c\langle\ell_c^J\rangle + N_s\langle\ell_s^J\rangle\tilde{u}_{gal}\right)\right] \times\left[\frac{1}{\bar{j}_{J'}}\int dm\frac{dn}{dm}b(m)\left(N_c\langle\ell_c^{J'}\rangle + N_s\langle\ell_s^{J'}\rangle\tilde{u}_{gal}\right)\right]$. ⟶ 2h term
  - $P_{CO(J)\times CO(J')}^{shot} = \frac{1}{\bar{j}_J\bar{j}_{J'}}\int dm\frac{dn}{dm}\left[N_c\ell_c^J\ell_c^{J'} + N_s\ell_s^J\ell_s^{J'}\right]$ ⟶ shot noise

COxCIB

$$C_{\ell,\nu\times\nu'}^{CO(J)\times CIB} = \sum_{J=1}^{13}\int \frac{d\chi}{dz}\frac{dz}{\chi^2}\xi_{CIB,\nu}(z)\xi_{CO(J),\nu'}(z)P_{CO(J)\times CIB}(k)$$

For the COxCIB power spectrum I'm using my 2 populations CIB model (so 2 sets of HOD parameters) and an effective HOD for the CO population.

- $P_{\rm CO\times ET(LT)}^{\rm 1h}(k) = \frac{1}{\bar{n}_{\rm gal}^{\rm ET(LT)}}\cdot\frac{1}{\bar{j}_{\rm J}^{\rm CO}}\int dm\frac{dn}{dm}\left[\left(N_c^{\rm ET(LT)}N_s^{\rm CO}\ell_s^{\rm J} + N_s^{\rm ET(LT)}N_c^{\rm CO}\ell_c^{\rm J}\right)\tilde{u}_{\rm gal} + N_s^{\rm ET(LT)}N_s^{\rm CO}\ell_s^{\rm J}\tilde{u}_{\rm gal}^2\right]$, 1h term
- $P_{\rm CO\times ET(LT)}^{\rm 2h}(k) = P_{\rm mm}^{\rm lin}(k)\left[\frac{1}{\bar{n}_{\rm gal}^{\rm ET(LT)}}\int dm\frac{dn}{dm}b(m)N_{\rm gal}^{\rm ET(LT)}\tilde{u}_{\rm gal}\right] \times\left[\frac{1}{\bar{j}_{\rm J}^{\rm CO}}\int dm\frac{dn}{dm}b(m)\left(N_c^{\rm CO}\ell_c^{\rm J} + N_s^{\rm CO}\ell_s^{\rm J}\right)\tilde{u}_{\rm gal}\right]$ 2h term
- $P_{\rm CO\times ET(LT)}^{\rm shot}(k) = \frac{1}{\bar{n}_{\rm gal}^{\rm ET(LT)}}\cdot\frac{1}{\bar{j}_{\rm J}^{\rm CO}}\int dm\frac{dn}{dm}\left[N_c^{\rm ET(LT)}N_c^{\rm CO}\ell_c^{\rm J} + \frac{N_s^{\rm ET(LT)}N_s^{\rm CO}}{Ns^{\rm ET} + N_s^{\rm LT}}\ell_s^{\rm J}\right]$ shot noise

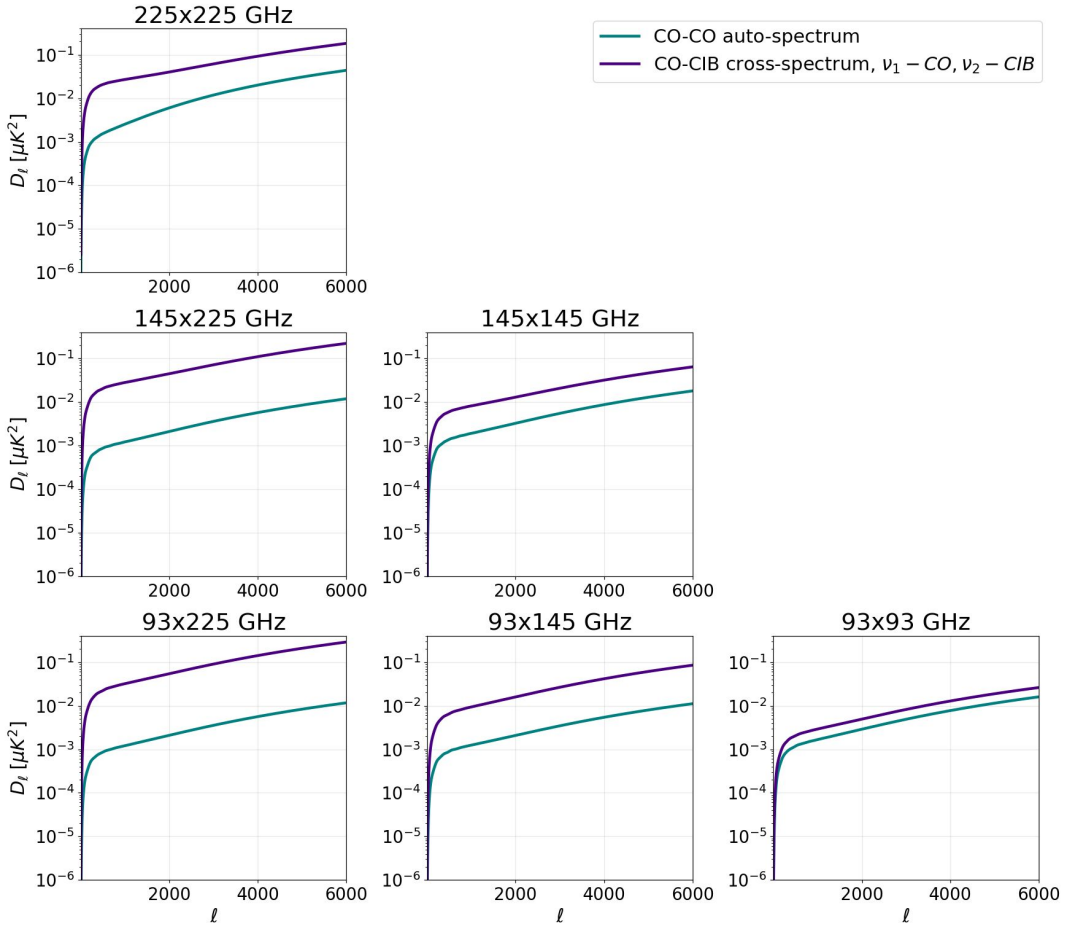
225x225 GHz
145x225 GHz
145x145 GHz
93x225 GHz
93x145 GHz
93x93 GHz
CO-CO auto-spectrum
CO-CIB cross-spectrum, $\nu_1 - CO, \nu_2 - CIB$
D_ℓ [μK^2]
ℓ

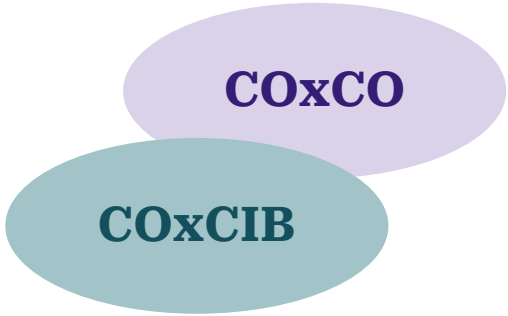
COxCO
COxCIB

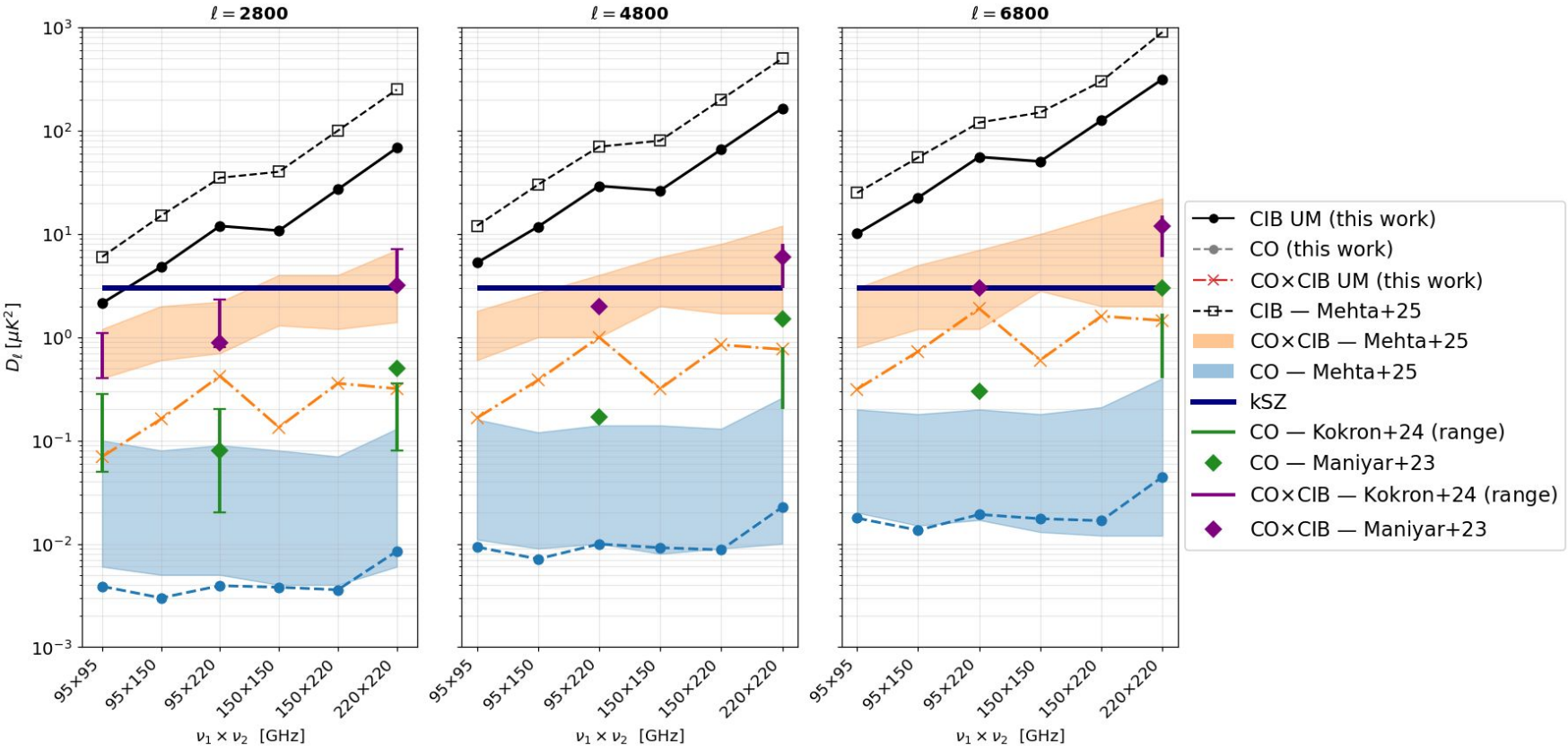
$\ell = 2800$
$\ell = 4800$
$\ell = 6800$
D_ℓ [μK^2]
10^3
10^2
10^1
10^0
10^{-1}
10^{-2}
10^{-3}
95×95
95×150
95×220
150×150
150×220
220×220
$\nu_1 \times \nu_2$ [GHz]
CIB UM (this work)
CO (this work)
CO×CIB UM (this work)
CIB — Mehta+25
CO×CIB — Mehta+25
CO — Mehta+25
kSZ
CO — Kokron+24 (range)
CO — Maniyar+23
CO×CIB — Kokron+24 (range)
CO×CIB — Maniyar+23